Accepted Manuscript

Iceberg Alley, East Antarctic Margin: Continuously laminated diatomaceous sediments from the late Holocene

Karen Alley, Kaylie Patacca, Jennifer Pike, Rob Dunbar, Amy Leventer

PII: S0377-8398(17)30099-3
DOI: https://doi.org/10.1016/j.marmicro.2017.12.002
Reference: MARMIC 1680

To appear in: *Marine Micropaleontology*

Received date: 22 June 2017
Revised date: 7 November 2017
Accepted date: 29 December 2017

Please cite this article as: Karen Alley, Kaylie Patacca, Jennifer Pike, Rob Dunbar, Amy Leventer , Iceberg Alley, East Antarctic Margin: Continuously laminated diatomaceous sediments from the late Holocene. The address for the corresponding author was captured as affiliation for all authors. Please check if appropriate. Marmic(2017), https://doi.org/10.1016/j.marmicro.2017.12.002

Iceberg Alley, East Antarctic Margin: Continuously laminated diatomaceous sediments from the late Holocene

Karen Alley[1, 2], Kaylie Patacca[1], Jennifer Pike[3], Rob Dunbar[4], Amy Leventer[1]

[1]Geology Department, Colgate University, Hamilton NY USA; kpatacca@colgate.edu; aleventer@colgate.edu

[2]present address: Geology Department, College of Wooster, Wooster OH USA; kalley@wooster.edu (corresponding author)

[3]School of Earth and Ocean Sciences, Cardiff University, Cardiff, Wales, UK; PikeJ@cardiff.ac.uk

[4]Department of Environmental Earth Systems Science, Stanford University, Stanford CA USA; dunbar@stanford.edu

Abstract:

A 24-meter jumbo piston core (NBP0101 JPC41) collected from an inner shelf basin in Iceberg Alley reveals an approximately 2000-year history of unusually high primary productivity. Iceberg Alley, an ~85 km long and 10-20 km wide cross-shelf trough on the Mac.Robertson Shelf, East Antarctica, reaches depths of 850 meters and is bounded on either side by shallow banks that are lined with grounded icebergs. The sediments are laminated on a mm- to cm-scale throughout and are highly biosiliceous. Microscopic examination of smear slides, quantitative diatom slides, and sediment thin sections reveals that the sediments are visually dominated by the diatom *Corethron pennatum*, a large and lightly silicified species notable for its long and narrow shape; the

valves, girdle bands and spines are all exceptionally well-preserved, suggesting rapid sedimentation. Other common species include sea ice-related *Fragilariopsis*, such as *F. curta* and *F. cylindrus*, with lesser contribution from other large diatoms, including *Rhizosolenia* spp. and *Chaetoceros* Ehrenberg subg. *Chaetoceros*. *Chaetoceros* Ehrenberg subg. *Hyalochaete* Gran resting spores, typically associated with large early-season blooms and common in many laminated sedimentary sections around the Antarctic margin, are surprisingly rare. Laminae with any significant terrigenous component are also very rare. Individual laminations appear to represent blooms, and in some cases sub-seasonal events are likely preserved. We suggest that this productive system is associated with the continuous presence of low-salinity meltwater derived from a combination of sea ice melt and grounded icebergs, which may be a source for a steady supply of micronutrients such as iron to the surface mixed layer.

Keywords: Diatoms; Southern Ocean; Holocene; Laminated sediments; East Antarctica

1. Introduction:

Diatoms in Antarctic sediments are powerful tools for paleoclimate reconstruction. The wide diversity of diatom species sensitive to changing oceanographic parameters such as water temperature, salinity, sea ice presence, and nutrient content allow for reconstruction of environmental and climatic conditions (Armand and Leventer, 2010). High rates of sediment accumulation in continental shelf troughs and basins, and in drift deposits may yield laminated records with annual or even seasonal resolution (Harris et al., 1999; Domack et al., 2001; Costa et al., 2007; Expedition 318 Scientists,

2011). Due to the excellent diatom preservation at many of these sites, diatom data have been instrumental in providing accurate reconstructions of local and regional climatic events, with the strength of interpretations dependent on a robust understanding of how the laminations formed. For example, studies of paired laminations in deglacial sediments from the western Antarctic Peninsula (Domack et al., 2005; Maddison et al., 2006; Leventer et al., 2002), Prydz Bay (Leventer et al., 2006), and the Mac.Robertson Shelf, East Antarctica (Stickley et al., 2005; Leventer et al., 2006) document the alternation of biosiliceous laminae, interpreted to have formed during periods of high productivity in spring and summer, followed by later season deposition of laminae containing greater terrigenous material and a more diverse diatom assemblage. These couplets record the short-lived formation of calving bay reentrants as ice retreated across the continental shelf at the end of the last glacial maximum.

Laminations observed in Holocene sediments at these sites, and others on the Antarctic shelf, also appear to record sub-seasonal to seasonal signals (Denis et al., 2006; Maddison et al., 2006; Crosta et al., 2007; Crosta et al., 2008; Denis et al., 2009; Maddison et al., 2012). However, their interpretation can be complicated by the insignificant abundance of terrigenous material, leaving changes in diatom assemblages as the sole signal of seasonal to inter-annual climatic and oceanographic change. In 2001, a jumbo piston core (NBP0101 JPC41) was collected from inner Iceberg Alley on the Mac.Robertson Shelf, East Antarctica (Fig. 1); the core comprises millimeter- to centimeter-scale laminations along its entire 24-meter length (Fig. 2). Like other high-resolution Antarctic margin post-deglaciation laminated records (Leventer et al., 2002; Denis et al., 2006; Maddison et al., 2006; Gregory, 2012; Maddison et al., 2012) , the

core lacks a significant percentage of terrigenous material, and is composed predominantly of diatom ooze laminations that vary greatly in thickness, texture, and sharpness of upper and lower boundaries. The diatom assemblage is visually dominated through most of the core by whole and broken valves and spines of *Corethron pennatum,* valves and setae of *Chaetoceros* Ehrenberg subg. *Chaetoceros*, and sea-ice-associated *Fragilariopsis*, especially *Fragilariopsis curta.* Other episodically common genera include *Rhizosolenia*.

In this study, we evaluate the role of deep cross-shelf trough geometry, the presence of icebergs grounded along the shallow banks that rim Iceberg Alley, and melting sea ice, in facilitating high primary productivity and subsequently high sediment accumulation rates. Microscopic evaluation of the the complex laminations in JPC41 indicates that high-resolution information from the late Holocene is preserved, but the record remains hard to interpret given difficulties in distinguishing an annually repeated pattern in the laminations and the likelihood that missing years occur. This study of inner Iceberg Alley sediments therefore provides the opportunity to learn about influences on diatom productivity at a high temporal resolution, and provides a framework for continued research.

2. Oceanographic Setting:

Iceberg Alley is located at approximately 63˚E, 67˚S on the Mac.Robertson Shelf, Mac.Robertson Land, just west of Prydz Bay and the Amery Ice Shelf (Fig. 1). The Mac.Robertson Shelf is moderately narrow and shallow (O'Brien et al., 1994; Harris and O'Brien, 1996). In most locations, metamorphic basement rock is covered by a relatively

thin veneer of sediments reflecting low sedimentation rates and the influence of currents and glaciations (O'Brien et al., 1994; Harris and O'Brien, 1996; Sedwick et al., 2001). Shallow banks divide deep basins and troughs as is typical of the Antarctic continental shelf (Taylor and McMinn, 2001). The deepest point on the Mac.Robertson Shelf is found in Nielsen Basin, which reaches ~1300 m (Leventer et al., 2006). Storegg Bank separates Nielsen Basin from Iceberg Alley to the west (O'Brien et al., 1994).

Iceberg Alley was carved across the Mac.Robertson Shelf during Quaternary glaciations, leaving a U-shaped trough with steep sides and a flat floor typical of glacial fjords. Iceberg Alley is about ~85 km long, 10-20 km wide and ~475-575 m deep, although some areas reach depths of 850 m (Leventer et al., 2006). Iceberg Alley receives its name from icebergs grounded at depths of 50-300 m that line both shallow banks (O'Brien et al., 1994; Stickley et al., 2005; Leventer et al., 2006). The geometry of troughs like Iceberg Alley traps sediment. Consequently, the deeper reaches of Iceberg Alley exhibit very high sedimentation rates (Stickley et al., 2005; Leventer et al., 2006).

Waters along the Mac.Robertson Coast are influenced at shallow depths (<200 m) by a westward-flowing Antarctic Coastal Current, with flow fastest along the outer shelf and slope, and slower on the inner shelf (O'Brien et al., 1994; Harris and O'Brien, 1998; O'Brien et al., 2014). Although some of this water mass continues along the shelf, much of the current is diverted offshore in the vicinity of Iceberg Alley (O'Brien et al., 1994; Taylor et al., 1997). Deeper waters north of this current are affected by Circumpolar Deep Water (CDW), which upwells onto the Mac.Robertson Shelf. This relatively warm water mass is modified and cools as it meets the waters of the westward-flowing Antarctic Coastal Current (Stickley et al., 2005). Although the shallow banks prevent the

modified CDW from intruding across the whole shelf, it is likely that it enters basins and troughs such as Iceberg Alley that cut through the shelf (Stickley et al., 2005). Wong and Riser (2013) also report the presence of modified shelf water on the Mac.Robertson slope; they observed cold, dense, and well-oxygenated bottom waters that may have the same source as Cape Darnley Bottom Water, to the east.

The Mac.Robertson Shelf is covered by sea ice for most of the year. Passive microwave data show that sea ice generally begins to break out in early summer, and open-water conditions generally dominate the shelf area by January, although breakouts during this time period varied from late December to early February (Spreen et al., 2008). However, sea ice is often trapped and held by the grounded icebergs on the shallow banks of Iceberg Alley, sometimes entirely precluding ice breakout during summer months (Taylor and McMinn, 2001). Over the past 15 years, For example, based on on-going satellite observations between 2002 and 2017, the ocean surface remained covered by sea ice through the summer season during 5 of those years (Spreen et al., 2008).

3. Materials and Methods:

3.1 Core sampling

Core NBP0101 JPC41 (67°07.829’S, 62 59.379’E, water depth 573 m) was collected aboard the RVIB *Nathaniel B. Palmer* in 2001 with a jumbo piston coring system. JPC41 is 24 meters long and exhibits laminations of highly biosiliceous sediments along its entire length. Photographs and x-ray images taken along the length of the core were used to identify a variety of distinct lamination styles. Thirteen 15-cm-long sections were sampled, chosen to include a representation of lamination types (Figure 2).

Some sections were overlapped to provide a longer continuous picture of depositional styles. The core sediments were sampled using a "cookie cutter" tool (Schimmelmann et al., 1990; Pike and Kemp, 1996). The tool, 15 cm long and 2 cm wide, was pressed into the sediments after slicing along its outline with a thin knife. A wire was used to loosen sediments from the bottom of the cutter, and the sliced section was rotated towards the edge of the core for removal. Samples were wrapped and refrigerated to prevent drying.

3.2 Thin section preparation

Thin sections were prepared from the sediment slabs following the method of Pike and Kemp (1996). Each cookie cutter section was cut in half along its length, and one half was set aside for archiving and other analyses. The remaining half of each section was cut into four segments, mitering the edges to provide overlap between the segments. These segments were placed in close-fitting, perforated boats made of aluminum foil, which were in turn placed in small plastic containers. Laboratory-grade acetone was pipetted into each container until the sediment samples were fully covered. Care was taken to avoid disturbing the sediments throughout the process. The acetone was removed and replaced with fresh acetone three times a day until fifteen exchanges were completed. This process effectively removed water from the samples without allowing them to dry and crack.

The samples were allowed to soak in the final acetone exchange for twelve hours before beginning to add resin. The final composition of the blocks used 46.8% TAAB Low Viscosity Resin, 50.8% VH2 Hardener, and 2.5% Accelerator. The mixture was gradually introduced by doing three replacements with a 3:2 resin-to-acetone ratio at

twelve-hour intervals, followed by two replacements at a ratio of 11:4, two at 13:2, and three using only the resin mixture. Analytical-grade acetone was used throughout this process.

The sediment samples were allowed to soak in the final resin mixture for four weeks. They were then cured for 24 hours at 30˚C, 45˚C, 60˚C and 90˚C with a twelve-hour cooling period between each step. The sediments embedded in the final resin blocks were prepared as thin sections on standard petrographic slides.

3.3 Smear slide and quantitative slide preparation

The retained cookie cutter halves were again divided in half along their lengths to provide two quarters, and one quarter was archived. Each of the other quarters was compared with core photos and x-ray images to determine the locations of lamination boundaries. Quarters were divided into laminations along these boundaries using a razor blade. Toothpick samples were taken from the center of each lamination, smeared onto coverslips, and adhered to glass slides with Norland Optical Adhesive cured under UV light.

The remainder of the lamination samples were then dried at 50°C. Quantitative slides were made using a settling method (Scherer, 1994). Between 5 and 10 mg of each sample was weighed out. Approximately 5 ml of water and hydrogen peroxide was added to each, and the samples were left on a warming tray for 2-3 days, allowing the peroxide to react with organic material and remove it from the sample. After reaction, the samples were placed in water-filled beakers and allowed to settle onto prepared coverslips over a

four hour period before the water was drained. As described above, the coverslips were mounted on glass slides using Norland Optical Adhesive #61 cured under UV light.

3.4 Microscopic analysis

Thin sections, smear slides, and quantitative slides were examined using light microscopy. Thin sections and smear slides were compared to create a qualitative record of changes in diatom assemblages through, and between, laminations. Quantitative slides were used for assessment of the diatom assemblage, by identification and counting of a minimum of 400 diatom valves along one or multiple cross-slide transects, at a magnification of 1000X. Counting followed the method described by Schrader and Gersonde (1978) and Crosta and Koc (2007). Diatom concentration (diatom valves per gram) and relative abundance (percentage) of diatom species were calculated (Scherer 1994). A total of 111 slides from nine 15-cm-long sections were counted as a way to evaluate overall changes in assemblages representative of observed laminations (numbered sections in Fig. 2; Assemblages illustrated in Fig. 5.1-5.9 and data available at http://www.usap-dc.org/ and in the Supplementary Data Table). In addition, biovolume estimates (Table 1) were made on six samples, three with high *Corethron pennatum* relative abundance, and three with high relative abundance of *Rhizosolenia* spp., based on data from Cornet-Barthaux et al. (2007) and Leblanc et al. (2012). To facilitate appropriate selection of biovolume data from the database (several options were available for some species), average valve dimension for *Corethron pennatum* was estimated based on measurement of 300 *Corethron* valve diameters, and for *Chaetoceros* Ehrenberg subg.

Hyalochaete Gran, a total of 50 valves and resting spores were measured, as described in Table 1.

3.5 Core chronology

Core chronology for JPC41 is based on three AMS radiocarbon dates (Table 2) of acid-insoluble organic matter analyzed at the Lawrence Livermore National Laboratory Center for Accelerator Mass Spectrometry (CAMS). Organic material from thick and uniformly light-colored laminae at the top, middle, and bottom of the core was selected and treated with 1N HCl wash on a hotplate at 95°C followed by multiple deionized water rinses. Ages were calibrated using CALIB Radiocarbon Calibration Program 7.1 (Stuiver et al., 2017); a local reservoir age of 1700±200 years was used, as previously assumed for other sites on the Mac.Roberston Shelf (Mackintosh et al., 2011).

4. Results and Discussion:

4.1 Core chronology

Based on the radiocarbon age model, the core spans ~1600 years in ~21 meters (Table 2). Loss of the most recent surface sediments during jumbo piston coring is a common occurrence, causing the projected age at the top of the core to be estimated at several hundred years old. The relationship between median calibrated age and sample depth indicates an accumulation rate rate of ~1.3 cm/year, described by the equation: [age (yrs before present) = 0.7663(depth (cm)) +340.5; R^2=0.99206]. Despite this linear relationship, accumulation rates are thought to vary widely, since lamination thicknesses observed in the core vary considerably, with some laminae suspected to represent single

years reaching thicknesses of ~10 cm (Fig. 3a). In addition, during five of the past 15 years (2002-2017), Iceberg Alley remained covered by sea ice (Spreen et al., 2008), preventing significant primary productivity and deposition, removing those years from the sediment record. Chirp 3.5 kHz sub-bottom profile data suggest that at least 85-90 meters of soft sediment can be found in inner Iceberg Alley. Together with the preliminary radiocarbon-based chronology, these data indicate that the inner Iceberg Alley site contains an extended very high-resolution record of paleoceanographic change throughout the Holocene.

4.2 Lamination styles

Core photos (Fig. 2) and x-ray images show that JPC41 is laminated continuously throughout its length. Laminations are differentiated by distinct color changes from light to dark orange-brown, with some boundaries that are abrupt and others that are more gradual. The core is highly biosiliceous, with an insignificant terrigenous component. Lamina thickness ranges from about 0.5-10 cm in thickness. The most common lamination style exhibits a gradual upwards transition in color from light to dark. The upper edge of these laminae typically shows an abrupt transition back to the lighter color sediment (Fig. 2, 3 and 4). The gradual change to a darker color is related to an increase in amorphous dark-colored material accompanied by a greater concentration of diatom fragments (Fig. 4). The light-colored sediment shows a much greater proportion of whole diatom valves such as the large, lightly silicified *Corethron pennatum*.

We suggest that the gradual change from light-colored sediment with whole diatoms to dark-colored sediment and diatom fragments represents the impacts of grazing

on the deposited assemblages, and that each of these gradual transitions represents a single year of deposition. Following the breakout of sea ice in the summer at this location, diatoms can quickly take advantage of available light and nutrients, beginning a period of high primary productivity. Initially, the summer bloom may be free from grazers, but over time the zooplankton population develops, feeding on the bloom, and causing selective shredding and fragmenting of the diatom cells (Smetacek et al., 2004) and the release of organic material as the products of grazing. This may account for the gradual change from whole diatoms to greater fragmentation and the presence of amorphous debris. When light levels decrease and sea ice re-forms in the fall, production and grazing is abruptly cut off. The cycle begins again with a fresh bloom the next time the sea ice breaks out, leading to the sudden change back to light-colored sediments.

In areas of high primary productivity, diatom blooms can be deposited rapidly, in mass sedimentation events that form visible laminae in the sediments (e.g., Smetacek, 1985; Alldredge and Gotschalk, 1989; Jordan et al., 1991; Sancetta et al., 1991; Crawford, 1995; Kemp et al., 2000; Hillenbrand et al., 2010). Many diatoms have characteristics that enhance aggregate formation, such as spines, that make entanglement more likely, and may lead to subsequent faster sedimentation (Smetacek, 1985; Alldredge et al., 1989; Riebesell, 1991). The development of a more heavily silicified resting spore or stage, as observed with species of *Chaetoceros* Ehrenberg subg. *Hyalochaete* Gran and *Eucampia antarctica*, also may result in rapid mass sinking (Smetacek, 1985; Salter et al., 2012).

High deposition rates found in Iceberg Alley generally appear to be sustained throughout the open water season. Although seasonal variations in diatom production

most likely occur, as documented in other modern Southern Ocean sites (Annett et al., 2010; Grigorov et al., 2014; Rembauville et al., 2015, 2016, Rigual-Hernandez et al., 2015, 2016), it is difficult to distinguish early- or late-season episodic diatom blooms within laminations. In addition, some layers, suspected to be annual, also exhibit visible sub-laminae, as shown in Fig. 3b, where a lamination thought to reflect a single year is interrupted by a dusky yellow layer dominated by *Rhizosolenia* spp. (Fig. 5.3). Similarly, the annual layer in Fig. 3c has visible color changes that are more distinct than the gradual background transition caused by increased grazing, but the origins of these layers are not clear from microscopic analysis. Further study in Iceberg Alley using sediment traps is needed to understand the nature of its productivity and depositional characteristics.

4.3 Diatom assemblages

Studies documenting diatom assemblages and downward flux in the modern Southern Ocean (Annett et al., 2010; Grigorov et al., 2014; Rembauville et al., 2015, 2016, Rigual-Hernandez et al., 2015, 2016) show that summer flux dominates, and that seasonality in assemblage composition and flux occurs. Analyses of diatom laminations in sediments from elsewhere around Antarctica, and other regions of the world ocean, also show that early and later season diatom assemblages can differ (Pike and Stickley, 2013). Documented early-season assemblages tend to be dominated by small diatoms such as *Chaetoceros* Ehrenberg subg. *Hyalochaete* Gran that can reproduce rapidly in nutrient-rich waters during the spring and summer and sink out as resting spores when nutrients near the surface are depleted (Hargraves and French, 1983; Leventer, 1991), a

process that can be important in bringing carbon to the sea floor (Rembauville et al., 2014, 2016). Fall assemblages tend to be composed of larger diatoms such as *Thalassiosira antarctica* resting spores and *Porosira glacialis* resting spores (Cunningham and Leventer, 1998; Stickley et al., 2005; Maddison et al., 2006, 2012; Pike et al., 2009), or *Rhizosolenia* spp., as part of the fall dump (Kemp et al., 2000).

The diatom data from JPC41 do not exhibit clear or consistent trends in seasonal progression of the diatom assemblage. Layers that are interpreted to be early-season (summer), based on color and the sharp contact with the underlying darker sediment, generally show a slightly higher percentage of *Corethron pennatum* than do the darker sediments that are interpreted to represent fall layers. This difference may reflect a combination of factors, including the composition of the living assemblage, the lightly silicified nature of *Corethron pennatum* that allows it to break easily, and potential fragmentation during grazing, although due to the presence of long spines this species may be more resistant to grazers (section 4.6).

Samples throughout the core are characterized by a numerical dominance of *Fragilariopsis curta*, averaging 45% relative abundance. Samples may also be co-dominated by *Chaetoceros* Ehrenberg subg. *Hyalochaete* Gran vegetative cells and resting spores (up to 40%) or *Fragilariopsis cylindrus* (generally <5% but reaching >60%). Diatoms such as *Corethron pennatum* (up to ~20%), *Rhizosolenia* spp. (up to ~20%), or other *Fragilariopsis* spp. (averaging ~20%) contribute a smaller but sizeable percentage. A few samples, however, show extremely high percentages of diatoms such as *F. cylindrus* and *Rhizosolenia* spp. The quantitative diatom data reveal the difficulty in using the visual character of the sediment to distinguish either annual or sub-annual

events as consistent changes are not clear. Because few coherent trends or defined assemblages can be identified within the quantitative diatom concentration data, the implications of diatom species that appear in significant percentages are addressed individually.

4.4 *Fragilariopsis curta* and *Fragilariopsis cylindrus*

Fragilariopsis curta is a dominant species in a majority of the slides from JPC41 with a relative abundance averaging 45%. *Fragilariopsis curta* is closely associated with sea ice, and its range is confined within winter sea ice extent around Antarctica (Armand et al., 2005). For this reason, it is mostly found near the coast, commonly occurring in waters characterized by recent sea ice melt, and may be associated with both pack ice and fast ice (e.g., Leventer, 1998; Leventer et al. 2002; Armand et al. 2005; Grigorov et al., 2014). Relative percentages of *F. curta* generally range from ~25% to ~60% in the samples analyzed. Exceptions occur, most notably for example at ~1579 cm which is dominated by *F. cylindrus,* and *F. curta* relative abundance reaches only 6% (Fig. 5.4).

Like *Fragilariopsis curta, Fragilariopsis cylindrus* is also associated with sea ice, and is most common in areas where winter sea ice is strongly consolidated and present for more than 7.5 months per year (Armand et al., 2005). It is found with both pack ice and fast ice in the adjacent sea ice edge zone (Garrison, 1991; Kang and Fryxell, 1992; Leventer, 1998). The abundance of *F. cylindrus* in JPC41 is highly variable, generally ranging from <3-15%. Striking exceptions occur, with very low relative contributions of *F. cylindrus* (0.2-0.5%) from ~1005-1007 cm (Figure 5.2) within a light-colored *Rhizosolenia* spp. lamina and relatively high % *F. cylindrus*, including peaks of 24% at

511.5 cm (Figure 5.1), 27% at 1016-1019 cm (Figure 5.2), 22% at 1263 cm (Figure 5.3) (associated with a *Corethron pennatum* bloom), 57% at 1579 cm (Figure 5.5) (a *Rhizosolenia* spp. sub-lamina), and 24% at 1899 cm. It is unclear why the relative abundance of *F. cylindrus* varies so dramatically, with several short-lived peaks. Photophysiologic studies suggest that *F. cylindrus* is successful at high light levels and variable or low iron concentrations (Kropuenske et al., 2010; Alderkamp et al., 2012; Petrou et al., 2012), but more work is needed to distinguish ecological controls on species of *Fragilariopsis*.

Several other species of *Fragilariopsis* (Armand et al., 2005) are common in JPC41, averaging moderately consistent relative abundances between 15-20%. This group is comprised of *Fragilariopsis obliquecostata, Fragilariopsis rhombica, Fragilariopsis ritscheri, Fragilariopsis separanda, Fragilariopsis sublinearis,* and *Fragilariopsis vanheurckii*. Due to the lack of a consistent distribution of any of these species in JPC41, it is difficult to understand their relationships to one another.

4.5 Large diatoms: *Corethron pennatum and Rhizosolenia* spp.

Corethron pennatum is a centric species common throughout Antarctic waters, occurring as very large, solitary cells (Fryxell and Hasle, 1971; mean cell biovolume and cell carbon biomass data summarized in Cornet-Barthaux et al., 2007 and Leblanc et al., 2012). Entanglement of *C. pennatum* to form mats is aided by a set of long spines on each valve as well as a set of shorter barbed spines (Crawford and Hinz, 1995) and the production of mucus that acts to bind mats together (Fryxell and Hasle, 1971).

JPC41 is visually dominated along the majority of its length by *Corethron pennatum*, as a combination of whole and broken valves, girdle bands and spines. However, although *C. pennatum* dominates visual qualitative analyses of the laminae, its numerical contribution to quantitative relative abundance is generally low, reaching a maximum in the section from 2152-2158 cm (Figure 5.8), where a broad peak reaches 33%. In the sections from 503-519 cm (Figure 5.1) and 1005-1019 cm (Figure 5.2), the relative abundance of *C. pennatum* is consistently < 2%. Biovolume estimates (Table 1) from three of the samples with highest relative abundance of *C. pennatum* demonstrate the much greater contribution of this species to the assemblage than suggested, with its contribution to biovolume from 71-92%, in samples where relative abundance ranges from only 17-34%. Maddison et al. (2012), in a study from the Dumont d'Urville Trough, East Antarctic Margin, similarly note that *C. pennatum* often does not constitute a large percentage of quantitative diatom analyses because the large, lightly silicified, elongate cells tend to break easily. This leads to bias in relative abundance counts since fragments < 1/2 valve are not counted during quantitative analyses. In addition, only valves are counted, not the numerous girdle bands that comprise this "drinking-straw" shaped species.

Rhizosolenia spp. also are relatively large diatoms (Cornet-Barthaux et al., 2007; Leblanc et al., 2012) common in the Southern Ocean, with an apical axis often >100 μm (Armand and Zielinski, 2001; Scott and Marchant, 2005). While most commonly associated with open ocean conditions, they are adaptable and also may tolerate areas characterized by sea ice presence (Stickley et al., 2005). Kemp et al. (2006) showed that giant diatoms, such as species of *Rhizosolenia*, are also prone to concentration along

major oceanic frontal zones. Similar to *C. pennatum*, *Rhizosolenia* spp. are frequently fragmented in sediment assemblages, often with only valve apices preserved (Armand and Zielinski, 2001).

In seasonally laminated sediments, *Rhizosolenia* spp. are commonly seen after the initial early-season bloom deposit and persist throughout the summer laminae (e.g., Stickley et al., 2005; Denis et al., 2006; Maddison et al., 2012). The first appearance in the spring or summer is thought to coincide with the strengthening of water column stratification, when warmer surface temperatures and/or low salinity meltwater creates a stronger thermocline/pycnocline (Pike and Stickley, 2013). Since *Rhizosolenia* spp. have a tendency to be very sensitive to water agitation, they die and are rapidly deposited when fall/winter mixing occurs (Kemp et al., 2000). *Rhizosolenia* spp. are present in generally low abundances, but visually dominate several isolated thin laminae, identified in core photos by a distinctive dusky yellow coloration, and very abrupt boundaries consistent with an interpretation of mass sedimentation (Fig. 3). The dominance of *Rhizosolenia* spp. in these layers points to very rapid settling, with fragile girdle bands as well as valves present in the sediments. In addition, like *C. pennatum*, *Rhizosolenia* spp. have a "drinking-straw" shape, developed by the many girdle bands between the two valves; the relative percentage data for these species often underestimates their importance. Biovolume estimates presented in Table 1 suggest a greater role of these groups in bringing silica to the seafloor even when not numerically dominant, with relative abundances of 8-18% equivalent to biovolume contributions of 80-96% in the selected samples.

4.6 Large diatoms and ocean stratification

Many studies show that both *Rhizosolenia* spp. and *Corethron pennatum* are capable of adjusting their buoyancy to move vertically through the water column (e.g., Crawford, 1995; Villareal et al., 1996; McKay et al., 2000; Richardson et al., 1996; Singler, 2005). The adaptation means that these large diatoms can acquire nutrients at depth beneath the pycnocline and return to the surface to photosynthesize, thereby avoiding competition for nutrients in oligotrophic surface waters. Leventer et al. (2002) suggest that this ability may make large diatoms like *C. pennatum*, as well as *Rhizosolenia* spp., best suited to strongly stratified conditions. The persistent abundance of *C. pennatum* in JPC41 sediments also may reflect a degree of grazer protection afforded by its barbs (Smetacek et al., 2004).

Abundant nutrients in the surface waters of Iceberg Alley, perhaps partially sourced from freshly upwelled iceberg meltwater, could provide the necessary nutrient supply to sustain blooms of large diatoms without requiring both water column stratification and migration. However, *Corethron pennatum* and *Rhizosolenia* spp. may have physiological restrictions requiring them to gather nutrients from deeper in the water column. Villareal et al. (1996) noted that the size of *Rhizosolenia* spp. introduces a surface-to-volume ratio such that the physiological processes of the cell are slowed. In effect, this means that the large *Rhizosolenia* spp. cells are at a disadvantage when competing for nutrients with smaller diatoms in surface waters.

We suggest that *Corethron* species may also find an advantage in migrating below the stratified surface layer where small diatoms rapidly take up nutrients, to a zone of lower competition deeper in the water column. This scenario may be likely for Iceberg

Alley, as summer meltwater, from both melting sea ice and nearby grounded icebergs, results in a shallow, low-salinity mixed layer. It also offers a mechanism for sustaining the large blooms of *Corethron pennatum* seen in JPC41 that are accompanied by a large and diverse assemblage of smaller diatoms (Fig. 5). Segregating species vertically in the water column in relation to nutrient uptake could allow for more efficient use of nutrients and support more diverse and abundant diatom species.

It is unclear what causes the sporadic laminae characterized by *Rhizosolenia* spp. that are found in JPC41. Goldman (1993) suggests that episodic addition of nutrients by wind events or other mixing mechanisms may cause abrupt blooms of large diatoms to occur. Several studies suggest that *Rhizosolenia* are associated with meltwater events (Jordan and Pudsey, 1992; Seeburg-Elverfeldt et al., 2004). The fact that *Rhizosolenia* spp. and *Corethron pennatum* generally are not observed to co-occur (Fig. 5) suggests that they respond differently to changing nutrient balances or have varying sensitivities to water agitation.

4.7 *Chaetoceros* Ehrenberg subg. *Hyalochaete* Gran

Species of *Chaetoceros* Ehrenberg subg. *Hyalochaete* Gran are found throughout the world's oceans, with high abundances associated with nutrient-rich sites of high primary productivity (Donegan and Schrader, 1982; Leventer, 1991; Karpuz and Jansen, 1992; Crosta et al., 1997; Zielinski and Gersonde, 1997; Armand et al., 2005). Cells from this subgenus tend to be relatively small, with an average apical axis < 20 μm (Scott and Marchant, 2005), and are able to grow quickly at shallow depths, making them suited to rapid blooms in areas rich in surface nutrients (Kemp et al., 2000; Grimm et al., 1997).

Many species of these small *Chaetoceros* Ehrenberg subg. *Hyalochaete* Gran form robust resting spores as a survival mechanism when surface nutrients are depleted (Hargraves and French, 1983; Kuwata et al., 1993). These resting spores rapidly flocculate following the bloom and settle to the seafloor in mass sedimentation events (Alldredge et al., 1993; Grimm et al., 1997) that can be important in the delivery of carbon to the sea floor (Rembauville et al., 2016).

In studies of laminated sediments, identification of early-season laminae is often assisted by the presence of high concentrations and relative abundances of *Chaetoceros* Ehrenberg subg. *Hyalochaete* Gran vegetative cells and/or resting spores (e.g., Leventer et al., 1996; Leventer et al., 2002; Denis et al., 2006; Maddison et al., 2012; Stickley et al., 2005). *Chaetoceros* Ehrenberg subg. *Hyalochaete* Gran, known to overwinter in sea ice (Ligowski et al., 1992, 2012), may seed the water column when cells are released from melting sea ice, leading to the early-season blooms of this subgenus observed in Southern Ocean shelf waters. In Iceberg Alley, as sea ice begins to melt in the summer, previously upwelled nutrients and nutrient input from melting ice, as well as water column stability promoted by low salinity meltwater, may promote large early-season diatom blooms. As the bloom progresses nutrients become depleted, inducing resting spore formation, resulting in mass sinking events of the more heavily silicified resting spores (Rembauville et al., 2016). In varved sediments observed from several sites around the Antarctic margin, including outer Iceberg Alley, nearly monospecific layers of *Chaetoceros* Ehrenberg subg. *Hyalochaete* Gran, dominated by resting spores, comprise the biogenic part of the varved couplet (Leventer et al., 2002; Maddison et al., 2005; Stickley et al., 2005; Leventer et al., 2006). These varved sediments are interpreted to

have formed during deglaciation, within a calving bay reentrant setting, characterized as highly productive systems associated with well-stratified, nutrient-rich surface waters (Leventer et al., 2006).

In contrast, *Chaetoceros* Ehrenberg subg. *Hyalochaete* Gran comprise, on average, only about 15% of the diatom assemblage in sediments from JPC41 (Fig. 5). Higher relative abundances, with values reaching up to about 40%, may signify the initiation of primary production; however, even in these intervals, vegetative valves are more common than resting spores. The laminations observed in JPC41 clearly reflect high primary productivity in the overlying surface waters, yet differ significantly from the varved sediments described from a calving bay reentrant setting. Inner Iceberg Alley sediments have a much less abundant *Chaetoceros* Ehrenberg subg. *Hyalochaete* Gran contribution to the diatom assemblage, lack the dominance of resting spores over vegetative valves, and lack a terrigenous component.

The question of why *Chaetoceros* Ehrenberg subg. *Hyalochaete* Gran blooms and the associated downward flux of resting spores are not characteristic of inner Iceberg Alley, when they are so common at other seemingly similar sites of rapid biosiliceous accumulation, is difficult to answer. Since *Chaetoceros* Ehrenberg subg. *Hyalochaete* Gran form resting spores when surface nutrients are depleted (Leventer, 1991; Kemp et al., 2000), we suggest the possibility that persistently high nutrient concentration in waters of inner Iceberg Alley may exceed that which would drive the resting spore formation. In addition, the relative paucity of *Chaetoceros* Ehrenberg subg. *Hyalochaete* Gran may reflect a system in which freshwater input precludes the deep convection needed to re-seed cells to the upper water column.

4.8 *Chaetoceros* Ehrenberg subg. *Chaetoceros*

Chaetoceros Ehrenberg subg. *Chaetoceros* is composed of relatively large-celled species. The two species most common in this study, *Chaetoceros criophilus* and *Chaetoceros dichaeta*, have apical axes up to 50 µm and long, hollow spines filled with chloroplasts (Tomas, 1997). The hollow spine morphology is interpreted as an adaptation that increases the surface area to volume ratio, and may enhance nutrient uptake rates (Smetacek et al., 2002). In addition, the large size and spines may serve as a protection against metazoan grazers and thus lead to the persistence and accumulation of these large *Chaetoceros* in the water column over a season (Smetacek et al., 2002).

In about half of the thin sections analyzed in JPC41, the diatom assemblage data record episodic delivery of *Chaetoceros* Ehrenberg subg. *Chaetoceros* to the sediments. For example, the light-colored, cottony-textured appearance of the sediments from 514-518 cm (Fig. 5.1) has nearly 20% *Chaetoceros* Ehrenberg subg. *Chaetoceros*. In the section from 1252-1267 cm (Fig. 5.3), a progression from domination by *Corethron pennatum* (1260-1267 cm) to *Chaetoceros* Ehrenberg subg. *Chaetoceros* (1258-1260 cm) and then to *Chaetoceros* Ehrenberg subg. *Hyalochaete* Gran (1255 cm) is recorded. Based on the visual appearance of the laminations, the sharp lower contact of the *C. pennatum* layer suggests it is an early-season bloom; the *Chaetoceros* Ehrenberg subg. *Chaetoceros* appear to reflect deposition of an accumulating population at the end of the summer. A similar pattern is observed in the section from 1552-1582 cm (Fig. 5.4), where sediments with higher abundances of *Corethron pennatum* transition to *Chaetoceros* Ehrenberg subg. *Chaetoceros* and, in this case, back to *C. pennatum* again.

The seasonal importance of changes in assemblage are difficult to interpret, but in each case the sharp lower boundary of the *C. pennatum* layer suggests initiation of an early-season bloom, with *Chaetoceros* Ehrenberg subg. *Chaetoceros* deposition likely at the end of the open-water season.

4.9 *Fragilariopsis kerguelensis*

Fragilariopsis kerguelensis is considered an open-ocean species, not typically found in areas where sea ice is present during summer months (Crosta et al., 2005). Its strong affinity with open water causes it to be negatively correlated with sea ice (Burckle, 1972), and many authors have used it as a proxy for open water (e.g., Crosta et al., 2007; Leventer, 1992). *F. kerguelensis* strongly dominates sediments deposited beneath the Antarctic Circumpolar Current (ACC) (Hamm et al., 2003), and in the paleo-record *F. kerguelensis* has been used to identify areas that have been influenced by the ACC (Leventer, 1992).

Fragilariopsis kerguelensis is present in only extremely low relative abundances in all of the slides studied apart from depths of 512-518 cm (~730 yBP) (Fig. 5.1) where abundances >10% are observed, and reach a high of 19%. This interval of the core also is unusual in that it is characterized by an almost complete absence of *Corethron pennatum*, which comprises only 1% of the assemblage in this interval. This is in contrast to other intervals where *C. pennatum* abundances are both more variable and generally higher, but *F. kerguelensis* is nearly absent (Fig. 5.2-5.9).

Iceberg Alley is influenced at depth by Circumpolar Deep Water (Stickley et al., 2005). During the deposition of sediment from 512-518 cm, this water mass may have

been more influential, and responsible for the higher relative contribution of *Fragilariopsis kerguelensis* to the diatom assemblage. The lack of *Corethron pennatum* indicates that the circulation change adversely affected conditions for this taxa, perhaps by lessening the strength of water column stratification. A more detailed assessment of changes in the contribution of *F. kerguelensis* to the diatom assemblage in inner Iceberg Alley sediments and nearby areas is recommended for the future, given the role of incursions of Circumpolar Deep Water over the Antarctic continental shelf in driving grounding line retreat (for example, Jenkins et al., 2010; Jacobs et al., 2012).

4.10 Controls on productivity

The rapidly accumulating biosiliceous sediments observed in inner Iceberg Alley reflect some combination of high primary productivity in the upper water column and concentration at the seafloor via sediment focusing within the deep depositional basin. We suggest that the high diatom flux reflects a combination of several factors. First, the high rates of diatom productivity in inner Iceberg Alley likely are facilitated by the presence of a stable water column (Arrigo et al., 1999). The development of this stratification is the result of freshwater input from melting sea ice (Vernet et al., 2008; Leventer et al., 1996); this is supported by the dominance of *Fragilariopsis curta* and other sea ice associated *Fragilariopsis* species. A stable water column in Iceberg Alley also may be facilitated by the sea floor morphology: a long, linear channel bounded by large icebergs that are grounded on the shallow banks lining the deep trough. Summertime melting of these grounded icebergs may add freshwater to the system throughout the diatom productivity season. In addition, wind mixing may be limited, at

times, within the open water region protected by the two lines of icebergs, one line on each side of Iceberg Alley.

The icebergs that give Iceberg Alley its name also may serve as a source of bioavailable iron. Glaciers collect terrigenous material and wind-borne dust for long periods of time before calving off into the ocean as icebergs. As these glacially-derived icebergs melt, they release the iron-laden terrigenous material into the water (Smith et al., 2007; Cefarelli et al., 2011; Vernet et al., 2012). Large icebergs may reach to depths well below the photic zone, where phytoplankton are unable to utilize available nutrients. However, as an iceberg melts, fresh, low-density meltwater upwells along the sides of the iceberg. In the process, local nutrient-laden saltwater is entrained in the upwelling and brought into the photic zone, facilitating greater primary productivity (Helly et al., 2011; Smith et al., 2007). Studies of modern free-floating icebergs have revealed diverse associated diatom assemblages (Cefarelli et al., 2011). Studies by Smith et al. (2007; 2011) on a free-floating iceberg in the Weddell Sea revealed an assemblage dominated in the larger fraction by *Corethron pennatum*, and secondarily by *Chaetoceros* Ehrenberg subg. *Chaetoceros* (Cefarelli et al., 2011; Vernet et al., 2011), similar to the assemblages found in JPC41. Iron fertilization experiments have typically induced large phytoplankton blooms dominated by diatoms, however, the dominant diatom species vary greatly depending on the site of the experiment (Assmy et al., 2007). Tsuda et al. (2003) suggest that the response population after iron enrichment is strongly influenced by the current ecosystem and the presence of a seed population of fast-growing diatoms that can quickly take advantage of added micronutrients.

The diatom assemblage observed in inner Iceberg Alley sediments may be best explained by Quéguiner (2013), who divided diatoms that develop in high-nutrient, iron-rich ocean areas into two groups: Group 1 that have lightly silicified fast growing cells that are homogeneously distributed in the surface water mixed layer; and Group 2 that have strongly silicified slowly growing cells within discrete layers in the water. The sediments in inner Iceberg Alley may record the co-occurrence of these two groups. Small *Chaetoceros* Ehrenberg subg. *Hyalochaete* Gran are identified as Group 1 diatoms, reflecting early summer blooms. Group 2 diatoms are dominated by the larger *Chaetoceros* Ehrenberg subg. *Chaetoceros, Corethron pennatum*, and *Rhizosolenia* spp. These large diatoms may survive well in lower light levels and their populations may progressively build throughout the polar spring and summer, with grazing-dependent mortality limited by their size and shape (Smetacek et al., 2004). In the case of inner Iceberg Alley, we hypothesize that a well-stratified water column with high iron input, both related to the persistent presence of sea- and glacial-ice meltwater, may be an ideal setting for the development and accumulation of large of blooms of these unusual diatom assemblages.

Further investigation is required to determine what factors control the unusual and persistently high rates of primary productivity in inner Iceberg Alley. In particular, the specific control on which of the major species or groups of species (*Corethron pennatum* versus *Chaetoceros* Ehrenberg subg. *Chaetoceros* versus *Rhizosolenia* spp.) are dominant is not well understood. However, based on previous studies, it is likely a combination of direct iron input, upwelling of entrained nutrient-laden water due to iceberg grounding beneath the photic zone, and a stable water column due to trough geometry and sea ice

and iceberg melt together creating the necessary conditions for very high diatom productivity and sedimentation rates.

5. Conclusions:

Sediments from NBP0101 JPC41, inner Iceberg Alley, show that this region experienced extremely high primary productivity during the late Holocene, yielding a high-resolution sediment record with annual and sub-annual laminae. The average sediment accumulation rate is ~1.3 cm/yr, however, some annual layers may be up to 10 cm thick, indicating that persistent sea ice presence may have prevented deposition in many years. If the average accumulation rate has not changed significantly since ice retreat following the last glacial maximum, inner Iceberg Alley could hold ~140 m of Holocene sediments.

Core JPC41 is highly biosiliceous and laminated throughout. Annual laminations are determined based on a gradual sediment color change from light to dark, representing a change from whole diatoms to fragmented diatoms accompanied by free organic material, a result of a gradual increase in grazing. Abrupt transitions from dark back to light sediment indicate a switch from fall to summer, though multiple years may be represented by a single transition. Sub-annual laminae may interrupt the gradual yearly transition.

Corethron pennatum visually dominates the core based on thin section analysis, however, *Fragilariopsis curta*, along with several other sea-ice associated *Fragilariopsis* species, typically dominate in terms of quantitative relative abundance. The overall diatom assemblage reflects an area with significant sea ice and spring-summer sea ice

and glacial ice meltwater, however, the increased abundance of the species *F. kerguelensis*, typically associated with the permanently open ocean zone (Crosta et al., 2005), in the uppermost interval analyzed may record the increased influence of the ACC at that time, approximately 730 yr BP.

Other important diatoms observed episodically include *Chaetoceros* Ehrenberg subg. *Chaetoceros*, as well as *Rhizosolenia* spp. Unlike varved sediments from the Antarctic margin that were deposited during deglacial time periods, the laminations in inner Iceberg Alley do not have high concentrations of *Chaetoceros* Ehrenberg subg. *Hyalochaete* Gran resting spores, suggesting that nutrient limitation may not occur here. Large diatoms, such as *Corethron pennatum*, *Chaetoceros* Ehrenberg subg. *Chaetoceros*, and *Rhizosolenia*, may be abundant in Iceberg Alley sediments due to their ability to adjust their buoyancy and exploit nutrients at depth, as well as their resistance to grazing. These populations may undergo mass deposition in the fall. However, the specific growth habitat for each group is not well known, with potential differences in their tolerance to lower light levels, nutrient concentrations, and water column agitation.

The exceptionally high diatom productivity and deposition rates in Iceberg Alley are attributed to the continual presence of grounded iceberg and sea ice meltwater, stabilizing the upper water column and perhaps supplying essential micronutrients such as iron. To date, a relatively small percentage of JPC41 has been studied in detail. Insights provided by this study into the history of Iceberg Alley warrant future research efforts to answer questions about how this unusual environment has developed over millennial to sub-annual timescales.

6. Acknowledgements:

We thank Tom Gregory for advice on thin section preparation procedures, and Charlotte Sjunneskog and Steve Petrushak for their assistance in sampling the core. Caitlin Cunningham and Kara Vadman were invaluable throughout the slide preparation process. We thank the scientific party and crew of the RVIB *NB Palmer* cruise NBP0101. NSF OPP- 9909367 and -9909837 supported this project.

7. References:

Alderkamp, A.C., Kulk, G., Buma, A.G.J., Visser, R.J.W., van Dijken, G.L., Mills, M.M., and Arrigo, K.R., 2012. The effect of iron limitation on the photophysiology of *Phaeocystis antarctica* (Prymnesiophyceae) and *Fragilariopsis cylindrus* (Bacillariophyceae) under dynamic irradiance. Journal of Phycology, 48 (1), 45-59, doi:10.1111/j.1529-8817.2011.01098.x.

Alldredge, A., and Gotschalk, C., 1989. Direct Observations of the Mass Flocculation of Diatom Blooms - Characteristics, Settling Velocities and Formation of Diatom Aggregates. Deep-Sea Research Part I-Oceanographic Research Papers, 36 (2), 159–171, doi:10.1016/0198-0149(89)90131-3.

Alldredge, A., Passow, U., and Logan, B., 1993. The Abundance and Significance of a Class of Large, Transparent Organic Particles in the Ocean. Deep-Sea Research Part I: Oceanographic Research Papers, 40 (6), 1131–1140, doi:10.1016/0967-0637(93)90129-Q.

Annett, A.L., Carson, D.S., Crosta, X., Clarke, A., and Ganeshram, R.S., 2010. Seasonal progression of diatom assemblages in surface waters of Ryder Bay, Antarctica. Polar

Biology, 33, 13-29, doi:10.1007/s00300-009-0681-7.

Armand, L.K., and Zielinski, U., 2001, Diatom species of the genus *Rhizosolenia* from Southern Ocean sediments:distribution and taxonomic notes. Diatom Research. 16, 259-294, doi:10.1080/0269249X.2001.9705520.

Armand, L.K. and Leventer, A., 2010. Palaeo sea ice distribution and reconstruction derived from the geological record. In: *Sea Ice* (Eds. D. N. Thomas & G.S. Dieckmann, G.S.), pp. 469–530, Wiley-Blackwell Publishing Ltd, Oxford.

Armand, L.K., Crosta, X., Romero, O., and Pichon, J.-J., 2005. The biogeography of major diatom taxa in Southern Ocean sediments. Palaeogeography, Palaeoclimatology, Palaeoecology, 223 (1-2), 93–126, doi:10.1016/j.palaeo.2005.02.015.

Arrigo, K. R., Robinson, D. H., Worthen, D. L., Dunbar, R. B., DiTullio, G. R., VanWoert, M., and Lizotte, M. P., 1999. Phytoplankton Community Structure and the Drawdown of Nutrients and CO2 in the Southern Ocean. Science, 283, 5400, 365-367.

Assmy, P., Henjes, J., Klaas, C., and Smetacek, V., 2007. Mechanisms determining species dominance in a phytoplankton bloom induced by the iron fertilization experiment EisenEx in the Southern Ocean. Deep-Sea Research Part I: Oceanographic Research Papers, 54 (3), 340-362, doi:10.1016/j.dsr.2006.12.005.

Buffen, A., Leventer, A., Rubin, A., and Hutchins, T., 2007. Diatom assemblages in surface sediments of the northwestern Weddell Sea, Antarctic Peninsula. Marine Micropaleontology, 62 (1), 7–30, doi:10.1016/j.marmicro.2006.07.002.

Burckle, L.H., 1972. Diatom evidence bearing on the Holocene in the South Atlantic.

Quaternary Research. 2 (3), 323–326, doi:10.1016/0033-5894(72)90052-X.

Cefarelli, A.O., Vernet, M., and Ferrario, M.E., 2011. Phytoplankton composition and abundance in relation to free-floating Antarctic icebergs. Deep-Sea Research Part II: Topical Studies in Oceanography, 58 (11-12), 1436–1450, doi:10.1016/j.dsr2.2010.11.023.

Costa, E., Dunbar, R.B., Kryc, K.A., Mucciarone, D.A., Brachfeld, S., Roark, E.B., Manley, P.L., Murray, R.W., and Leventer, A., 2007. Solar forcing and El Niño Southern Oscillation (ENSO) influences on productivity cycles interpreted from a late Holocene high-resolution marine sediment record, Adélie Drift, East Antarctic Margin. U.S. Geological Survey and the National Academies, Short Research Paper 036, doi:10.3133/of2007-1047.srp036.

Crawford, R., 1995. The Role of Sex in the Sedimentation of a Marine Diatom Bloom. Limnology and Oceanography, 40 (1), 200–204, doi:10.4319/lo.1995.40.1.0200.

Crawford, R.M., and Hinz, F., 1995. The spines of the centric diatom *Corethron criophilum*: Light microscopy of vegetative cell division. European Journal of Phycology. 30 (2), 95–105, doi:10.1080/09670269500650861.

Crosta, X., Pichon, J.J., and Labracherie, M., 1997. Distribution of *Chaetoceros* resting spores in modern peri-Antarctic sediments. Marine Micropaleontology, 29, 283-299, doi.org/10.1016/S0377-8398(96)00033-3.

Crosta, X., and Koc, N., 2007. Diatoms: From micropaleontology to geochemistry. In: Developments in Marine Geology, Volume 1, DOI 10.1016/S1572-5480(07)01013-5.

Crosta, X., Romero, O., Armand, L., and Pichon, J., 2005. The biogeography of major diatom taxa in Southern Ocean sediments: 2. Open ocean related species.

Palaeogeography, Palaeoclimatology, Palaeoecology. 223, 66–92, doi:10.1016/j.palaeo.2005.03.028.

Crosta, X., Debret, M., Denis, D., Courty, M.A., and Ther, O., 2007. Holocene long- and short-term climate changes off Adélie Land, East Antarctica. Geochemistry Geophysics Geosystems, 8 (11), 1-15, doi:10.1029/2007GC001718.

Crosta, X., Denis, D., and Ther, O. 2008. Sea ice seasonality during the Holocene, Adelie Land, East Antarctica. Marine Micropaleontology, 66, 222-232, doi:10.1016/j.marmicro.2007.10.001.

Cunningham, W.L. and Leventer, A.R., 1998. Diatom assemblages in surface sediments of the Ross Sea, Antarctica: relationship to modern oceanographic conditions. Antarctic Science, 10(2), 134–146, doi:10.1017/S0954102098000182.

Denis, D., Crosta, X., Zaragosi, S., Romero, O., Martin, B., and Mas, V., 2006. Seasonal and subseasonal climate changes recorded in laminated diatom ooze sediments, Adelie Land, East Antarctica. The Holocene, 16 (8), 1137–1147, doi:10.1177/0959683606069414.

Denis, D., Crosta, X., Schmidt, S., Carson, D. S., Ganeshram, R. S., Renssen, H., Bout-Roumazeilles, Zaragosi, S., Martin, B., Cremer, M., and Giraudeau, J., 2009. Holocene glacier and deep water dynamics, Adelie Land region, East Antarctica. Paleoceanography, 28 (13-14), 1291-1303, doi:10.1029/2008PA001689.

Domack, E., Leventer, A., Dunbar, R., Taylor, F., Brachfeld, S., Sjunneskog, C., and ODP Leg 178 Science Party, 2001. Chronology of the Palmer Deep Site, Antarctic Peninsula: a Holocene paleoenvironmental reference for the circum-Antarctic. The Holocene, 11 (1), 1–9, *doi:*10.1191/095968301673881493.

Domack, E.W., Amblàs, D., Gilbert, R., Brachfeld, S., Camerlenghi, A., Rebesco, M., Canals, M., and Urgeles, R., 2005. Subglacial morphology and glacial evolution of the Palmer deep outlet system, Antarctic Peninsula. Geomorphology, 75 (1-2), 125–142, doi:10.1016/j.geomorph.2004.06.013

Donegan, D., and Schrader, H., 1982. Biogenic and abiogenic components of laminated hemipelagic sediments in the central Gulf of California. Marine Geology, 48 (3-4), 215-237, doi:10.1016/0025-3227(82)90098-6.

Expedition 318 Scientists, 2011. Site U1357. *In* Escutia, C., Brinkhuis, H., Klaus, A., and the Expedition 318 Scientists, Proc. IODP, 318: Tokyo (Integrated Ocean Drilling Program Management International, Inc.), doi:10.2204/iodp.proc.318.105.2011.

French, F. W. and Hargraves, P. E., 1985. Spore formation in the life cycles of the diaotms *Chaetoceros diadema* and *Leptocylindrus danicus*. Journal of Phycology, 21,477–483. doi:10.1111/j.0022-3646.1985.00477.x

Fryxell, G., and Hasle, G., 1971. *Corethron criophilum* Castracane, its distribution and structure (G. Llano & I. Wallen, Eds.). Biology of the Antarctic Seas IV, 17, 335–346.

Garrison, D., 1991. Antarctic Sea Ice Biota. American Zoologist, 31 (1), 17–33.

Goldman, J., 1993. Potential Role of Large Oceanic Diatoms in New Primary Production. Deep-Sea Research Part I-Oceanographic Research Papers. 40 (1), 159–168, doi:10.1016/0967-0637(93)90059-C.

Gregory, T., 2012. Holocene sea ice-ocean-climate variability from Adelie Land, East Antarctica, Ph.D. Dissertation, Cardiff University, 251 pp.

Grigorov, I., Rigual-Hernandez, A.S., Honjo, S., Kemp, A.E.S., and Armand, L.K.,

2014. Settling fluxes of diatom frustules to the interior of the Antarctic Circumpolar Current along 170°W. Deep Sea Research Part I, 93, 1-13.

Grimm, K., Lange, C., and Gill, A., 1997. Self-sedimentation of phytoplankton blooms in the geologic record. Sedimentary Geology, 110, 151–161.

Hamm, C., Merkel, R., Springer, O., Jurkojc, P., Maier, C., Prechtel, K., and Smetacek, V., 2003. Architecture and material properties of diatom shells provide effective mechanical protection. Nature, 421 (6925), 841–843, doi:10.1038/nature01416.

Hargraves, P.E. and French, F.W., 1983. Diatom resting spores: significance and strategies. In: G. Fryxell (Editor), Survival Strategies of the Algae. Cambridge University Press, Cambridge, pp. 49-68.

Harris, P., and O'Brien, P., 1996. Geomorphology and sedimentology of the continental shelf adjacent to Mac Robertson Land, East Antarctica: A scalped shelf. Geo-Marine Letters, 16 (4), 287–296, doi:10.1016/j.dsr2.2012.07.024.

Harris, P., and O'Brien, P., 1998. Bottom currents, sedimentation and ice-sheet retreat facies successions on the Mac.Robertson Shelf, East Antarctica. Marine Geology, 151 (1-4), 47-72, doi:10.1016/S0025-3227(98)00047-4.

Harris, P.T., Domack, E., Manley, P.L., Gilbert, R., and Leventer, A., 1999. Andvord drift: A new type of inner shelf, glacial marine deposystem from the Antarctic Peninsula. Geology, 27 (8), 683-686, doi: 10.1130/0091-7613(1999) 027<0683:ADANTO>.

Helly, J.J., Kaufmann, R.S., Stephenson, G.R., Jr., and Vernet, M., 2011. Cooling, dilution and mixing of ocean water by free-drifting icebergs in the Weddell Sea. Deep-Sea Research Part II: Topical Studies in Oceanography, 58 (11-12), 1346–1363,

doi:10.1016/j.dsr2.2010.11.010.

Hillenbrand, C.-D., Smith, J.A., Kuhn, G., Esper, O., Gersonde, R., Larter, R.D., Maher, B., Moreton, S.G., Shimmield, T.M., and Korte, M., 2010. Age assignment of a diatomaceous ooze deposited in the western Amundsen Sea Embayment after the Last Glacial Maximum. Journal of Quaternary Science, 25, 280-295.

Jacobs, S., Jenkins, A., Hellmer, H., Giulivi, C., Nitsche, F., Huber, B., and Guerrero, R., 2012. The Amundsen Sea and the Antarctic Ice Sheet. Oceanography, 25 (3),154–163, http://dx.doi.org/10.5670/oceanog.2012.90.

Jenkins, A., Dutrieux, P., Jacobs, S.S., McPhail, S.D., Perrett, J.R., Webb, A.T., and White, D., 2010. Observations beneath Pine Island Glacier in West Antarctica and implications for its retreat. Nature Geoscience, 3, 468-472, doi:10.1038/NGEO890.

Jordan, R.W., and Pudsey, C.J. 1992. High-resolution diatom stratigraphy of Quaternary sediments from the Scotia Sea. Marine Micropaleontology, 19 (3), 201-237.

Jordan, R.W., Priddle, J., Pudsey, C.J., Barker, P.F., and Whitehouse, M.J. 1991. Unusual diatom layers in Upper Pleistocene sediments from the northern Weddell Sea. Deep-Sea Research, 38 (7), 829-843.

Kang, S.H.-, and Fryxell, G.A., 1992. *Fragilariopsis cylindrus* (Grunow) Krieger: The most abundant diatom in water column assemblages of Antarctic marginal ice-edge zones. Polar Biology, 12, 609-627, doi:10.1007/BF00236984.

Karpuz, N.K., and Jansen, E., 1992. A high-resolution diatom record of the last deglaciation from the SE Norwegian Sea: documentation of rapid climatic changes. Paleoceanography 7 (4), 499– 520, doi:10.1029/92PA01651.

Kemp, A., Pike, J., Pearce, R., and Lange, C., 2000. The "Fall dump" - a new perspective

on the role of a "shade flora" in the annual cycle of diatom production and export flux. Deep-Sea Research Part II-Topical Studies in Oceanography. 47 (9-11) 2129–2154, doi:10.1016/S0967-0645(00)00019-9.

Kemp, A.E.S., Pearce, R.B., Grigorov, I., Rance, J., Lange, C.B., Quilty, P., and Salter, I., 2006. Production of giant marine diatoms and their export at oceanic frontal zones: implications for Si and C flux from stratified oceans. Global Biogeochemical Cycles, 20(4), GB4S04, doi:10.1029/2006GB002698.

Kropuenske, L.R., Mills, M.M., van Dijken, G.L., ALderkamp, A.-C., Berg, G.M., Robinson, D.H., Welschmeyer, N.A., and Arrigo, K.R., 2010. Strategies and rates of photoacclimation in two major Southern Ocean phytoplankton taxa: *Phaeocystis antarctica* (Haptophyta) and *Fragilariopsis cylindrus* (Bacillariophyceae). Journal of Phycology, 46, (6), 1138-1151, doi:10.1111/j.1529-8817.2010.00922.x.

Kuwata, A., Hama, T., and Takahashi, 1993. Ecophysiological characterization of two life forms, resting spores and resting cells, of a marine planktonic diatom, *Chaetoceros pseudocurvisetus*, formed under nutrient depletion. Marine Ecology Progress Series, 102, 245-255.

Leblanc, K., Arístegui, J., Armand, L., Assmy, P., Beker, B., Dode, A., Breton, E., Cornet, V., Gibson, J., Gosselin, M.-P., Kopczynska, E.E., Marshall, H.G., Peloquin, J.M., Piontkovski, S., Poulton, A.J., Queguiner, B., Schiebel, R., Shipe, R., Stefels, J., van Leeuwe, M.A., Varela, M., Widdicombe, C.E., and Yallop, A., 2012. A global diatom database - abundance, biovolume and biomass in the world ocean. Earth System Science Data, Copernicus Publications, 4 (1), pp.149-165, doi:10.5194/essd-4-149-2012.

Leventer, A., 1991. Sediment trap diatom assemblages from the northern Antarctic Peninsula region. Deep-Sea Research, 38 (8/9), 1127-1143, doi:10.1016/0198-0149(91)90099-2.

Leventer, A., 1992. Modern Distribution of Diatoms in Sediments From the George V Coast, Antarctica. Marine Micropaleontology, 19 (4), 315–332, doi:10.1016/0377-8398(92)90036-J.

Leventer, A., 1998. The fate of sea ice diatoms and their use as paleoenvironmental indicators. *In*: American Geophysical Union Antarctic Research Series 73, Antarctic Sea Ice: Biological Processes, Lizotte, M.P. and Arrigo, K.R. (eds.), pp. 121-137.

Leventer, A., and Dunbar, R., 1996. Factors influencing the distribution of diatoms and other algae in the Ross Sea. Journal of Geophysical Research. 101 (C8), 18,489-18,500, doi:10.1029/96JC00204.

Leventer, A., Dunbar, R., and DeMaster, D., 1993. Diatom evidence for late Holocene climatic events in Granite Harbor, Antarctica. Paleoceanography, 8 (3), 373-386, doi:10.1029/93PA00561.

Leventer, A., Domack, E.W., Ishman, S., Brachfeld, S., McClennen, C., and Manley, P., 1996. Productivity cycles of 200-300 years in the Antarctic Peninsula region: Understanding linkages among the sun, atmosphere, oceans, sea ice, and biota. Geological Society of America Bulletin. 108 (12), 1626–1644, doi:10.1130/0016-7606(1996)108<1626:PCOYIT>2.3.CO;2.

Leventer, A., Domack, E.W., Barkoukis, A., McAndrews, B., and Murray, J., 2002. Laminations from the Palmer Deep: a diatom-based interpretation. Paleoceanography, 17 (2), 1-15, doi:10.1029/2001PA000624.

Leventer, A., Domack, E.W., Dunbar, R., Pike, J., Stickley, C., Maddison, E., Brachfeld, S., Manley, P., and McClennen, C., 2006. Marine sediment record from the East Antarctic margin reveals dynamics of ice sheet recession. GSA Today, 16 (12), 4-10, doi:10.1130/GSAT01612A.1.

Ligowski R., Godlewski M., Łukowski A., 1992. Sea ice diatoms and ice edge planktonic diatoms at the northern limit of the Weddell Sea pack ice. Proc. NIPR Symp. *Polar Biology*, 5, 9-20.

Ligowski, R., Jordan, R.W., and Assmy, P., 2012. Morphological adaptation of a planktonic diatom to growth in Antarctic sea ice. Marine Biology, 159, 817-827, doi: 10.1007/s00227-011-1857-6.

Mackintosh, A., Golledge, N., Domack, E., Dunbar, R., Leventer, A., White, D., Pollard, D., DeConto, R., Fink, D., Zwartz, D., Gore, D., and Lavoie, C., 2011. Retreat of the East Antarctic ice sheet during the last glacial termination. Nature Geoscience, 4 (2011), 195-202, doi:10.1038/ngeo1061.

Maddison, E., Pike, J., Leventer, A., Dunbar, R., Brachfeld, S., Domack, E.W., and Manley, P., 2006. Post-glacial seasonal diatom record of the Mertz Glacier Polynya, East Antarctica. Marine Micropaleontology, 60 (1), 66–88, doi:10.1016/j.marmicro.2006.03.001.

Maddison, E.J., Pike, J., and Dunbar, R., 2012. Seasonally laminated diatom-rich sediments from Dumont d'Urville Trough, East Antarctic Margin: Late-Holocene Neoglacial sea-ice conditions. The Holocene, 22 (8), 857-875, doi:10.1177/0959683611434223.

Maddison, E.J., Pike, J., Leventer, A., and Domack, E.W, 2005. Deglacial seasonal and

sub-seasonal diatom record from Palmer Deep, Antarctica. Journal of Quaternary Science, 20 (5), 435–446, doi:10.1002/jqs.947.

McKay, R., Villareal, T., and La Roche, J., 2000. Vertical migration by *Rhizosolenia* spp. (Bacillariophyceae): Implications for Fe acquisition. Journal of Phycology, 36 (4), 669–674, doi:10.1046/j.1529-8817.2000.99125.x.

O'Brien, P.E., Truswell, E.M., and Burton, T., 1994. Morphology, Seismic Stratigraphy and Sedimentation History of the Mac. Robertson Shelf, East Antarctica. Terra Antarctica. 1 (2), 407–408.

O'Brien, P.E., Harris, P.T., Post, A.L., and Young, N., 2014. East Antarctic continental shelf: Prydz Bay and the Mac.Robertson Land Shelf. in: Continental Shelves of the World: Their Evolution During the Last Glacio-Eustatic Cycle. Geological Society, London, Memoirs, 41, 241-254. Chocci, F.L. and Chivas, A.R. (eds).

Petrou, K., Kranz, S.A., Doblin, M.A., and Ralph, P.J., 2012. Photophysiological responses of *Fragilariopsis cylindrus* (Bacillariophyceae) to nitrogen depletion at two temperatures. Journal of Phycology, 48 (1), 127-136, doi:10.1111/j.1529-8817.2011.01107.x.

Pike, J. and Kemp, A.E.S., 1996. Preparation and analysis techniques for studies of laminated sediments. In: A.E.S. Kemp (Editor), Palaeoclimatology and Palaeoceanography from laminated sediments. Geological Society, Special Publication 116, 37-48, doi:10.1144/GSL.SP.1996.116.01.05.

Pike, J., Crosta, X., Maddison, E.J., Stickley, C.E., Denis, D., Barbara, L., Renssen, H., 2009. Observations on the relationship between the Antarctic coastal diatoms *Thalassiosira antarctica* Comber and *Porosira glacialis* (Grunow) Jørgensen and sea

ice concentrations during the Late Quaternary. Marine Micropaleontology, 73, 14–25, doi.org/10.1016/j.marmicro.2009.06.005.

Pike, J., and Stickley, C.E., 2013. Diatom fossil records from marine laminated sediments. in: Encyclopedia of Quaternary Science, ed. S. A. Elias, Elsevier, 554-561.

Quéguiner, B., 2013. Iron fertilization and the structure of planktonic communities in high nutrient regions of the Southern Ocean. Deep-Sea Research II, 90, 43-54, doi:10.1016/j.dsr2.2012.07.024.

Rembauville, M., Blain, S., Armand, L., Quéguiner, B., and Salter, I., 2015. Export fluxes in a naturally iron-fertilized area of the Southern Ocean – Part 2: importance of diatom resting spores and faecal pellets for export. Biogeosciences 12, 3171–3195. http://dx.doi.org/10.5194/bg-12-3171-2015.

Rembauville, M., Manno, C., Tarling, G.A., Blain, S., and Salter, I., 2016. Strong contribution of diatom resting spores to deep-sea carbon transfer in naturally iron-fertilized waters downstream of South Georgia. Deep-Sea Research I, 115, 22-35, doi:10.1016/j.dsr.2016.05.002.

Richardson, T., Ciotti, A., Cullen, J., and Villareal, T., 1996. Physiological and optical properties of *Rhizosolenia formosa* (Bacillariophyceae) in the context of open-ocean vertical migration. Journal of Phycology, 32 (5), 741–757, doi:10.1111/j.0022-3646.1996.00741.x.

Rigual-Hernàndez, A.S., Trull, T.W., Bray, S.G., Cortina, A. and Armand, L.K., 2015. Latitudinal and temporal distributions of diatom populations in the pelagic waters of the Subantarctic and Polar Frontal Zones of the Southern Ocean and their role in the

biological pump. Biogeosciences, 12, 5309-5337, doi.org/10.5194/bg-12-5309-2015.

Rigual-Hernàndez, A.S., Trull, T.W., Bray, S.G., and Armand, L.K., 2016. The fate of diatom valves in the Subantarctic and Polar Frontal Zones of the Southern Ocean: Sediment trap versus surface sediment assemblages. Palaeogeography, Palaeoclimatology, Palaeoecology, 457, 129-143, doi.org/10.1016/j.palaeo.2016.06.004.

Riebesell, U., 1991. Particle aggregation during a diatom bloom. II. Biological aspects. Marine Ecology Progress Series, 69, 281-291.

Salter, I., Kemp, A.E.S., Moore, C.M., Lampitt, R.S., Wolff, G.A., and Holtvoeth, J., 2012. Diatom resting spore ecology drives enhanced carbon export from a naturally iron-fertilized bloom in the Southern Ocean. Glob. Biogeochem. Cycles 26, GB1014. http://dx.doi.org/10.1029/2010GB003977.

Sancetta, C., Villareal, T., and Falkowski, P., 1991. Massive Fluxes of Rhizosolenid Diatoms - a Common Occurrence. Limnology and Oceanography, 36 (7), 1452–1457, doi:10.4319/lo.1991.36.7.1452.

Scherer, R.P., 1994. A new method for the determination of absolute abundance of diatoms and other silt-sized sedimentary particles. Journal of Paleolimnology, 12 (1), 171-178, doi:10.1007/BF00678093.

Schimmelmann, A., Lange, C.B. and Berger, W.H., 1990. Climatically controlled marker layers Santa Barbara Basin sediments and fine-scale core-to-core correlation. Limnology and Oceanography, 35 (1), 165–173, doi:10.4319/lo.1990.35.1.0165.

Schrader, H. J., and Gersonde, R., 1978. Diatoms and silicoflagellates. In: A. Zachariasse, et al. (Eds), Micropaleontological counting methods and techniques — An exercise

on an eight meters section of the Lower Pliocene of Capo Rossello, Sicily. Utrecht Micropaleontology Bulletin, 17, 129–176.

Scott, F.J., and Marchant, H.J., 2005. Antarctic Marine Protists. Australian Biological Resources Study, Australian Antarctic Division, 563 pp.

Sedwick, P., Harris, P., Robertson, L., McMurtry, G., Cremer, M., and Robinson, P., 2001. Holocene sediment records from the continental shelf of Mac. Robertson Land, East Antarctica. Paleoceanography, 16 (2), 212–225, doi:10.1029/2000PA000504.

Seeberg-Elverfeldt, IA, Lange CB, Arz HW, Patzold J, and Pike J., 2004. The significance of diatoms in the formation of laminated sediments of the Shaban Deep, Northern Red Sea. Marine Geology, 209, 279-301.

Singler, H.R., 2005. Nitrogen inputs into the euphotic zone by vertically migrating *Rhizosolenia* mats. Journal of Plankton Research, 27 (6), 545–556, doi:10.1093/plankt/fbi030.

Smetacek, V.S., 1985. Role of sinking in diatom life-history cycles: ecological, evolutionary and geological significance. Marine Biology, 84 (3), 239–251.

Smetacek, V., Klaas, C., Menden-Deuer, S., and Rynearson, T.A., 2002. Mesoscale distribution of dominant diatom species relative to the hydrographical field along the Antarctic Polar Front. Deep-Sea Research II, 49 (18), 3835-3848, doi:10.1016/S0967-0645(02)00113-3.

Smetacek, V., Assmy, P. and Henjes, J., 2004. The role of grazing in structuring Southern Ocean pelagic ecosystem and biogeochemical cycles. Antarctic science, 16 (4), 541-558, doi:10.1017/S0954102004002317.

Smith, K.L., Jr, Robison, B.H., Helly, J.J., Kaufmann, R.S., Ruh, H.A., Shaw, T.J.,

Twinning, B.S., and Vernet, M., 2007. Free-drifting icebergs: hot spots of chemical and biological enrichment in the Weddell Sea. Science, 317 (5837), 478–482, doi: 10.1126/science.1142834.

Smith, K.L., Jr., Sherman, A.D., Shaw, T.J., Murray, A.E., Vernet, M., and Cefarelli, A.O., 2011. Carbon export associated with free-drifting icebergs in the Southern Ocean. Deep-Sea Research Part II: Topical Studies in Oceanography, 58 (11-12), 1485–1496, doi.org/10.1016/j.dsr2.2010.11.027.

Spreen, G., Kaleschke, L., and Heygster, G., 2008. Sea ice remote sensing using AMSR-E 89 Ghz channels. J. Geophys. Res., 113 (C02S03), doi:10.1029/2005JC003384.

Stickley, C.E., Pike, J., Leventer, A., Dunbar, W., Domack, E W, Brachfeld, S., Manley, P., and McClennan, C., 2005. Deglacial ocean and climate seasonality in laminated diatom sediments, Mac.Robertson Shelf, Antarctica. Palaeogeography, Palaeoclimatology, Palaeoecology, 227 (4), 290–310, doi:10.1016/j.palaeo.2005.05.021.

Stuiver, M., Reimer, P.J., and Reimer, R.W., 2017, CALIB 7.1 [WWW program] at http://calib.org, accessed 2017-4-9.

Taylor, F., and McMinn, A., 2001. Evidence from diatoms for Holocene climate fluctuation along the East Antarctic margin. The Holocene, 11 (4), 455–466, doi:10.1191/095968301678302896.

Taylor, F., McMinn, A., and Franklin, D., 1997. Distribution of diatoms in surface sediments of Prydz Bay, Antarctica. Marine Micropaleontology. 32 (3-4), 209–229, doi:10.1016/S0377-8398(97)00021-2.

Tomas, C.R., 1997. Identifying Marine Phytoplankton. Cambridge University Press, 858

pp.

Tsuda, A., Takeda, S., Saito, H., Nishioka, J., Nojiri, Y., Kudo, I., Kiyosawa, H., Shiomoto, A., Imai, K., Ono, T., Shimamoto, A., Tsumune, D., Yoshimura, T., Aono, T., Hinuma, A., Kinugasa, M., Suzuki, K., Sohrin, Y., Noiri, Y., Tani, H., Deguchi, Y., Tsurushima, N., Ogawa, H., Fukami, K., Kuma, K., and Saino, T., 2003. A Mesoscale Iron Enrichment in the Western Subarctic Pacific Induces a Large Centric Diatom Bloom. Science, 300 (5621), 958–961, doi:10.1126/science.1082000.

Vernet, M., Martinson, D., Iannuzzi, R., Stammerjohn, S., Kozlowski, W., Sines, K., Smith, R., and Garibotti, I., 2008. Primary production within the sea-ice zone west of the Antarctic Peninsula: I—Sea ice, summer mixed layer, and irradiance. Deep-Sea Research Part II: Topical Studies in Oceanography, 55 (18-19), 2068–2085, doi:10.1016/j.dsr2.2008.05.021.

Vernet, M., Sines, K., Chakos, D., Cefarelli, A.O., and Ekern, L., 2011. Impacts on phytoplankton dynamics by free-drifting icebergs in the NW Weddell Sea. Deep-Research II, 58 (11-12), 1422-1435, doi:10.1016/j.dsr2.2010.11.022.

Vernet, M., Smith, K.L. Jr., Cefarelli, A.O., Helly, J.J., Kaufmann, R.S., Lin, H., Long, D.G., Murray, A.E., Robison, B.H., Ruhl, H.A., Shaw, T.J., Sherman, A.D., Sprintall, J., Stephenson, G.R. Jr., Stuart, K.M., and Twining, B.S., 2012. Islands of ice: Influence of free-drifting Antarctic icebergs on pelagic marine ecosystems. Oceanography, 25 (3), 38–39, doi:10.5670/oceanog.2012.72.

Villareal, T., Woods, S., Moore, J., and Culver-Rymsza, K., 1996. Vertical migration of *Rhizosolenia* mats and their significance to NO_3-fluxes in the central north Pacific gyre. Journal of Plankton Research, 18 (7), 1103–1121.

Wong, A.P.S., and Riser, S.C., 2013. Modified shelf water on the continental slope north of Mac Robertson Land, East Antarctica. Geophysical Research Letters, 40 (23), 6186-6190, doi:10.1002/2013GL058125.

Zielinski, U., and Gersonde, R., 1997. Diatom distribution in Southern Ocean surface sediments (Atlantic sector): Implications for paleoenvironmental reconstructions. Palaeogeography, Palaeoclimatology, Palaeoecology, 129 (3-4), 213–250, doi:10.1016/S0031-0182(96)00130-7.

Figure Captions:

Figure 1: Study location, including the site of Jumbo Piston Core 41 (JPC41). Major currents are also shown. Adapted from Stickley et al. (2005).

Figure 2: Core photograph illustrating laminations and distribution of samples. Sections for which diatoms were counted are numbered and shown in black; sections from which thin sections were made by no slides were counted also are shown in black, but not numbered. Numbering corresponds to sections in Figure 5.

Figure 3: Lamination styles. A) A relatively homogeneous 10 cm interval of sediment, illustrating a very gradual transition from a lighter to darker colored, and an abrupt transition to a light-colored lamina. B) A similar gradual transition from lighter to darker color, interrupted by a *Rhizosolenia* sub-lamina centered at 1255 cm (also see Fig. 5c). C) A potentially more complex section of core, with several sub-laminae present. Up-core is to the left in all photos.

Figure 4: Core photo from ~2187-2196 cm depth, and thin section view centered at ~2192 cm, of the abrupt transition from a dark fall layer to a light-colored summer layer.

Note the presence of free dark-colored organic matter and abundant diatom fragments during fall, and the dominance of whole diatoms; in this image, primarily *Corethron pennatum* cells, in the spring.

Figure 5.1-5.9. Core photographs and diatom assemblage data for discrete sections of NBP0101 JPC41: 1) 503.6-518.4 cm, 2) 1005-1019.5 cm, 3) 1251.3-1265.8 cm, 4 & 5) 1551.8-1580.7 cm, 6) 1894-1909 cm, 7) 2122-2137.4 cm, 8) 2147.6-2163.5 cm, 9) 2187-2202 cm. Numbering corresponds to sections in Figure 2.

Table 1. Biovolume Estimates

Sample Depth (cm)				1559		2154		2187.5	
Taxa present >2%	V min (μm^3)	V max (μm^3)	V avg (μm^3)	relative %	% biovol.	relative %	% biovol.	relative %	% biovol.
Chaetoceros (Hyalochaete) veg[1]			522	2.8	0.1	11.8	0.2	12.8	0.4
Chaetoceros (Hyalochaete) RS[1]			277	0.9	0.0	12.8	0.1	12.8	0.2
Chaetoceros (Phaeoceros)[2]	16823	21630	19227	0.2	0.3	1.9	1.3	0.5	0.5
Corethron pennatum[3]	7069	134303	70686	**16.5**	**70.9**	**33.8**	**82.8**	**21.3**	**91.6**
Eucampia antarctica	1286	79627	40457	1.7	4.2	6.6	9.3	0.5	1.1
Fragilariopsis curta	96	1188	642	47.9	1.9	16.3	0.4	38.0	1.5
Fragilariopsis cylindrus	9	452	231	1.9	0.0	0.9	0.0	1.6	0.0
Fragilariopsis rhombica	484	5953	3219	4.7	0.9	1.4	0.2	0.9	0.2
Fragilariopsis ritscheri	22	9849	4936	2.6	0.8	4.7	0.8	3.4	1.0
Fragilariopsis sublinearis	22	9849	4936	4.3	1.3	0.9	0.2	0.7	0.2
Fragilariopsis vanheurckii	22	9849	4936	2.6	0.8	0.7	0.1	0.2	0.1
Fragilaropsis spp.[4]	22	9849	4936	3.4	1.0	0.5	0.1	2.5	0.8
Rhizosolenia spp.[5]	20358	318086	169222	1.3	13.2	0.7	4.2	0.2	2.4
Thalassiosira tumida	2425	56549	29487	2.6	4.6	0.5	0.5	0.0	0.0
TOTAL				93.2		93.6		95.4	

Sample Depth (cm)				506.75		1255		1579	
Taxa present >2%	V min (μm^3)	V max (μm^3)	V avg (μm^3)	relative %	% biovol.	relative %	% biovol.	relative %	% biovol.
Chaetoceros (Hyalochaete) veg[1]			522	1.9	0.0	4.9	0.1	3.2	0.1
Chaetoceros (Hyalochaete) RS[1]			277	4.2	0.0	3.0	0.0	2.7	0.0
Chaetoceros (Phaeoceros)[2]	16823	21630	19227	4.6	2.7	2.6	2.8	0.3	0.2
Corethron pennatum[3]	7069	134303	70686	0.8	1.7	0.9	3.4	0.5	1.1
Eucampia antarctica	1286	79627	40457	0.4	0.5	1.1	2.4	1.2	1.5
Fragilariopsis curta	96	1188	642	45.3	0.9	38.5	1.4	6.3	0.1
Fragilariopsis cylindrus	9	452	231	4.8	0.0	13.2	0.2	56.5	0.4
Fragilariopsis rhombica	484	5953	3219	1.7	0.2	2.3	0.4	1.2	0.1
Fragilariopsis ritscheri	22	9849	4936	0.4	0.1	1.5	0.4	2.2	0.3
Fragilariopsis sublinearis	22	9849	4936	2.3	0.4	5.1	1.4	2.4	0.4
Fragilariopsis vanheurckii	22	9849	4936	0.8	0.1	0.9	0.2	0.5	0.1
Fragilaropsis spp.[4]	22	9849	4936	3.1	0.5	4.3	1.2	0.7	0.1
***Rhizosolenia* spp.**[5]	20358	318086	169222	**17.1**	**89.7**	**8.5**	**80.8**	**18.2**	**95.6**
Thalassiosira tumida	2425	56549	29487	3.5	3.2	3.2	5.3	0.0	0
TOTAL				90.9		89.8		95.8	

Biovolume estimates from Leblanc et al. (2012) except for *Chaetoceros (Hyalochaete)* from Cornet-Barthaux et al. (2007).
Species >2% in any of the 6 selected samples are considered here.
Samples selected for high relative contribution of either *Corethron pennatum* or *Rhizosolenia* spp.

[1]Given the many entries for *Chaetoceros (Hylaochaete)* in Leblanc et al. (2012)
we measured the pervalvar (P), apical (A) and transapical (T) axes in specimens from the 2187.5 cm sample.
A total of 50 specimens were measured, 20 resting spores (A and P) and 30 vegetative (A and T) valves.
Resting spores, average A = 10 µm, average P = 7 µm; Vegetative valves, average A = 12 µm, average T = 8 µm.
These data are close to those presented in Cornet-Barthaux et al, (2007); so we utilized their biovolume estimates.

[2]Most *Chaetoceros (Phaeoceros)* identified as *Chaetoceros dichaeta*.

[3]Leblanc et al. (2012) present several biovolume estimates for *Corethron pennatum*, dependent on average valve diameter.
Average biovolume was selected based on the average of measurements of 100 valve diameters
in each of the three samples with high % *Corethron pennatum* presented here.
1559 cm average = 35 µm; 2154 cm average = 33 µm; 2187.5 cm average = 34 µm;
consequently used 30 µm diameter data from Leblanc et al. (2012)

[4]*Fragilariopsis* spp. includes *F. kerguelensis*, *F. obliquecostata*, *F. separanda* and unidentified *Fragilariopsis* spp.

[5]*Rhizosolenia* spp. not identified to species level in all counts.
In five samples with high relative abundance of *Rhizosolenia*, 100 specimens were identified to species level. Results:
78-87% *R. antennata* f. *semispina*, 5-13% *Rhizosolenia* sp. A from Armand and Zielinski (2001)
(probably *R. hebetata* f. *semispina* as illustrated in Scott and Marchant, 2005), 0-15% *Rhizosolenia antennata* f. *antennata*.

[6]Percent biovolume =100* (% relative abundance * V avg)/Total biovolume

Table 2. Radiocarbon dates from core NBP0101 JPC41

Sample depth (cm)	**^{14}C age (years)**	**Corr error (years)**	**Median probable age (years B.P.)**
102-103	2055	106	384
1339-1340	3195	104	1451
2225-2226	3665	104	1997

Highlights:

Late Holocene continuously laminated marine sediment from East Antarctic shelf

Role of meltwater from icebergs and sea ice in driving blooms of diatoms

Potential for high resolution paleoclimate records from inner shelf basin Antarctica

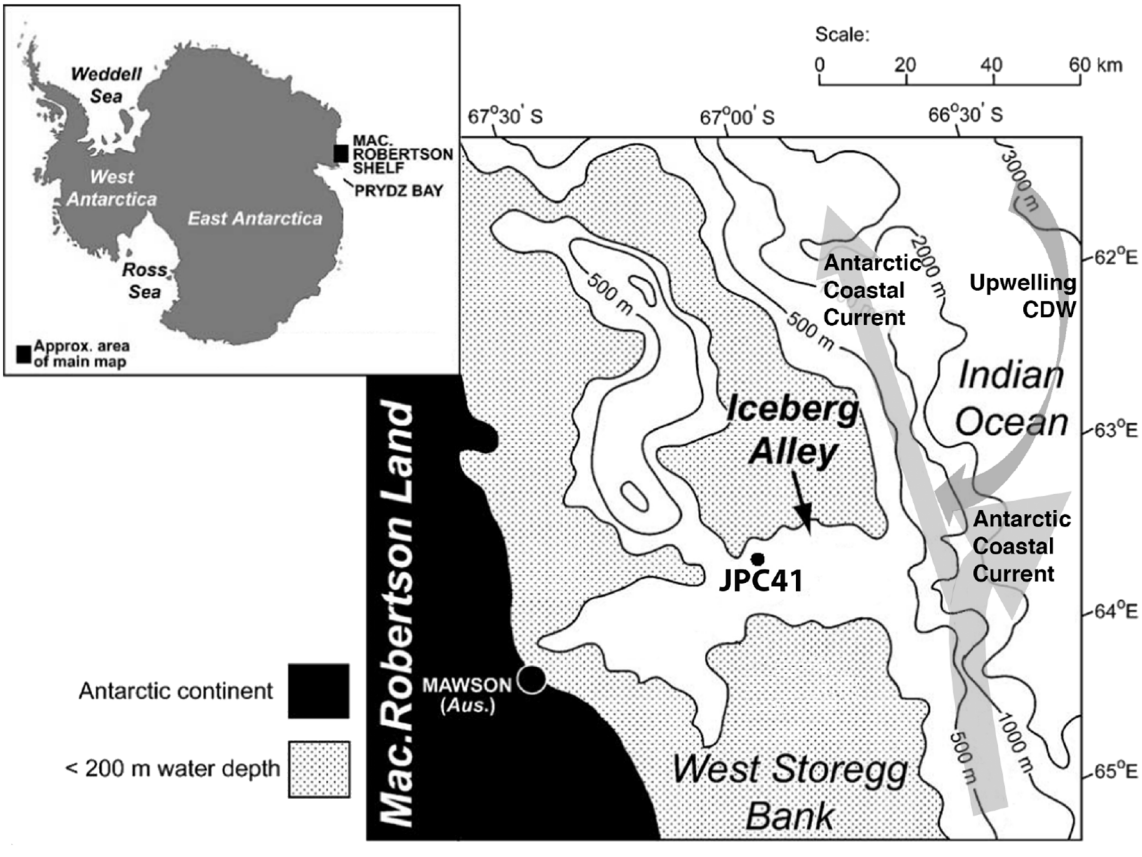
Weddell Sea
West Antarctica
East Antarctica
Ross Sea
MAC. ROBERTSON SHELF
PRYDZ BAY
Approx. area of main map
Scale:
0 20 40 60 km
67°30' S
67°00' S
66°30' S
62°E
63°E
64°E
65°E
3000 m
2000 m
500 m
500 m
500 m
1000 m
Antarctic Coastal Current
Upwelling CDW
Indian Ocean
Iceberg Alley
JPC41
Antarctic Coastal Current
Mac.Robertson Land
MAWSON (Aus.)
West Storegg Bank
Antarctic continent
< 200 m water depth

Figure 1

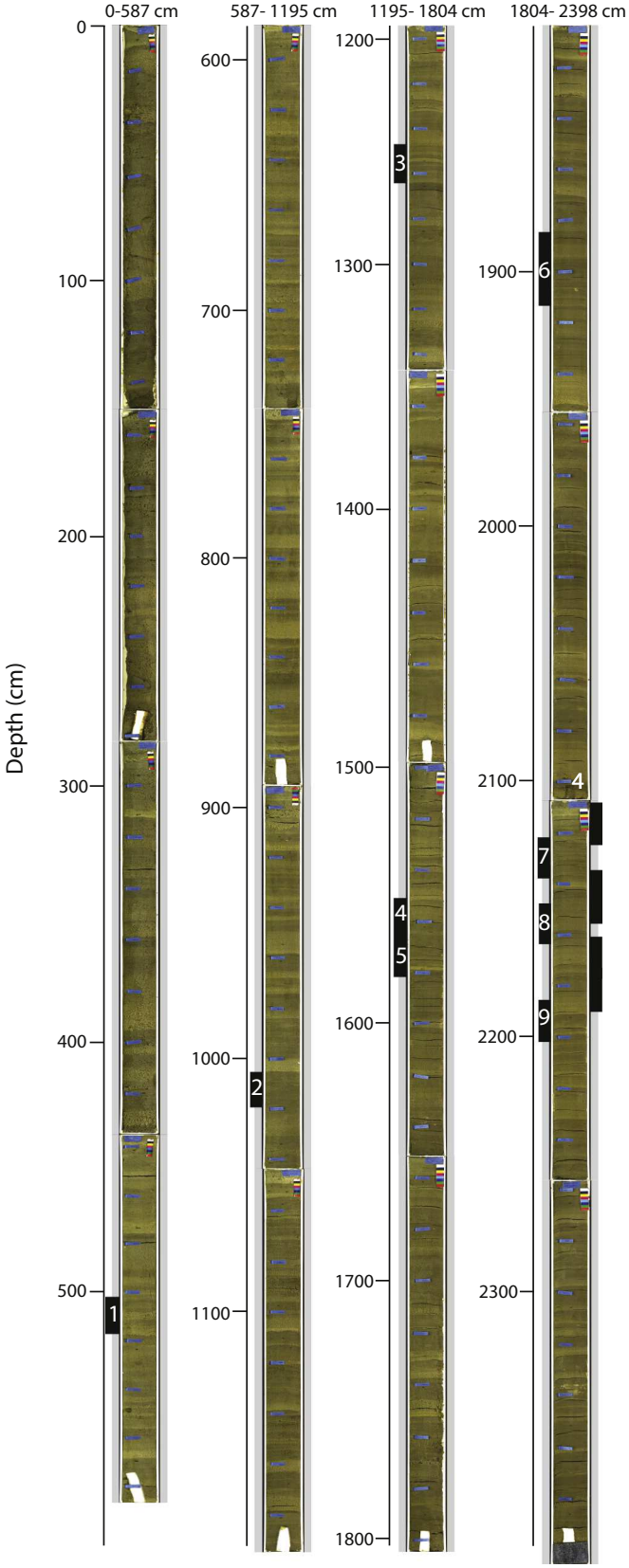
0-587 cm
587- 1195 cm
1195- 1804 cm
1804- 2398 cm
Depth (cm)
0
100
200
300
400
500
600
700
800
900
1000
1100
1200
1300
1400
1500
1600
1700
1800
1900
2000
2100
2200
2300
1
2
3
4
5
6
7
8
9

Figure 2

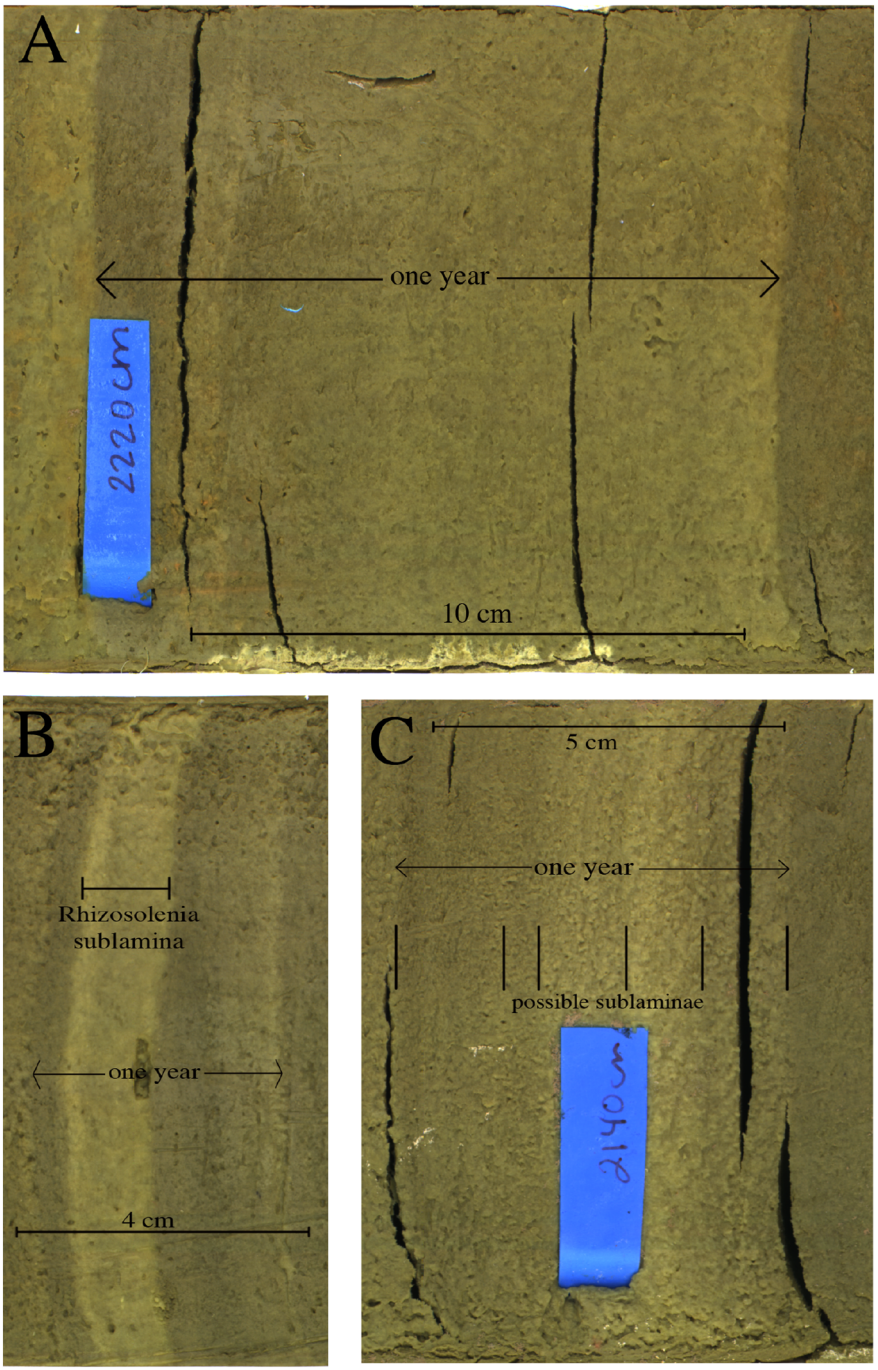
A
one year
2220 cm
10 cm
B
Rhizosolenia
sublamina
one year
4 cm
C
5 cm
one year
possible sublaminae
2220 cm

Figure 3

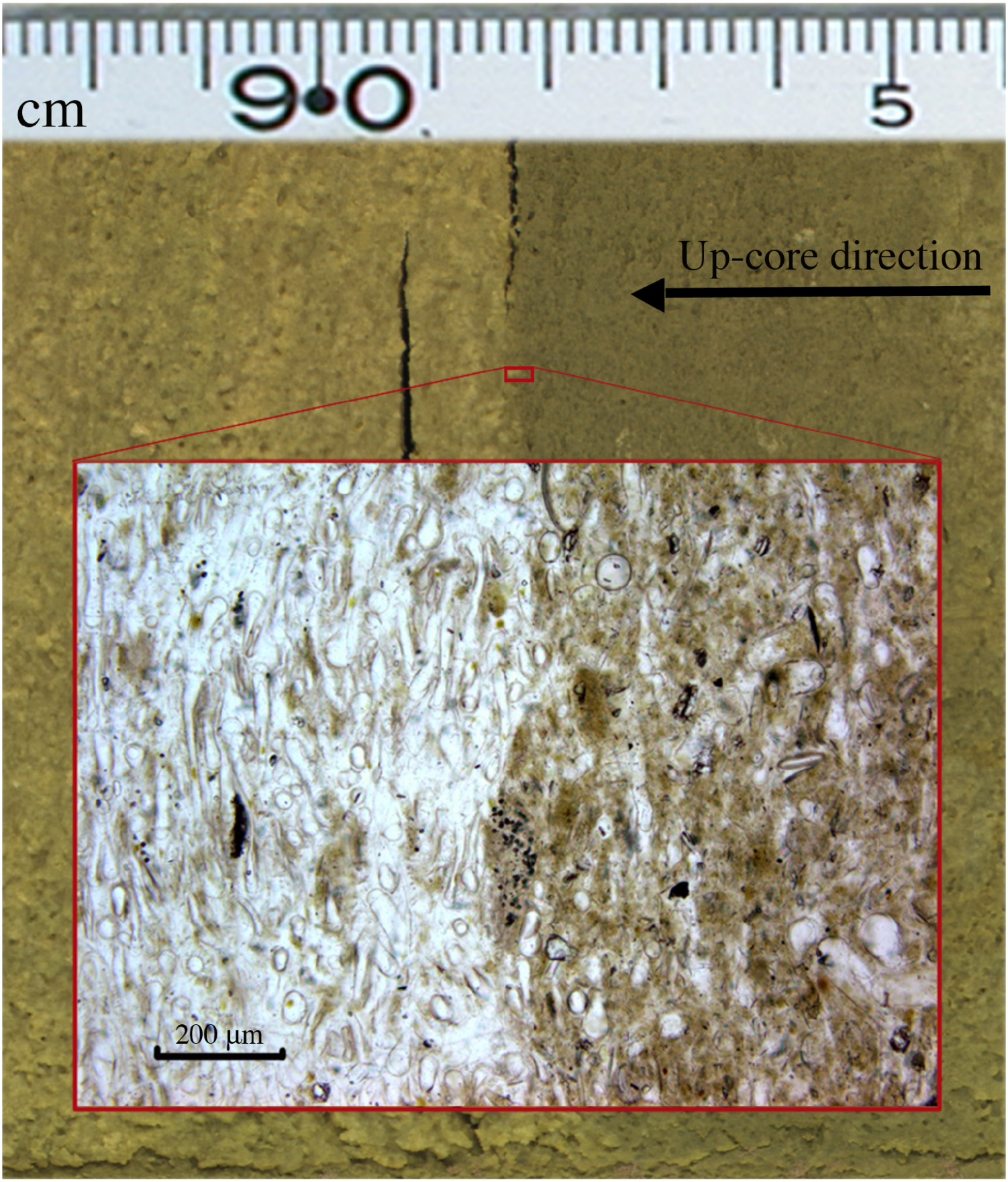

Figure 4

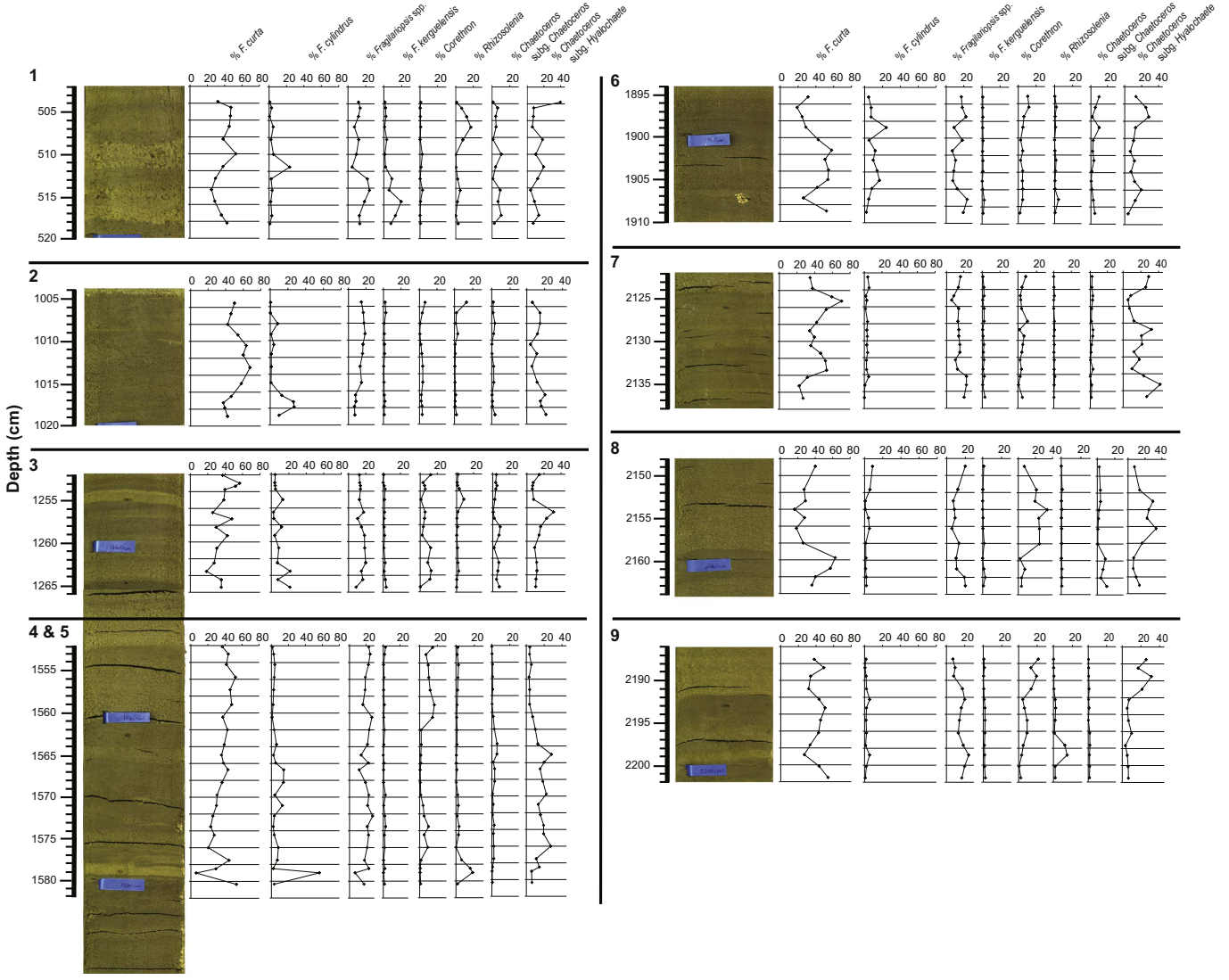
% F. curta
% F. cylindrus
% Fragilariopsis spp.
% F. kerguelensis
% Corethron
% Rhizosolenia
% Chaetoceros subg. Chaetoceros
% Chaetoceros subg. Hyalochaete
Depth (cm)
1
2
3
4 & 5
6
7
8
9

Figure 5